NAVAL POSTGRADUATE SCHOOL

Monterey, California

THESIS

EVALUATION OF THE NAVAL RESEARCH LABORATORY LIMITED AREA DYNAMICAL WEATHER PREDICTION MODEL: TOPOGRAPHIC AND COASTAL INFLUENCES ALONG THE WEST COAST OF THE UNITED STATES

by

Frank J. Grandau
March 1992

Thesis Advisor: Teddy R. Holt

Approved for public release; distribution is unlimited

DISCLAIMER NOTICE

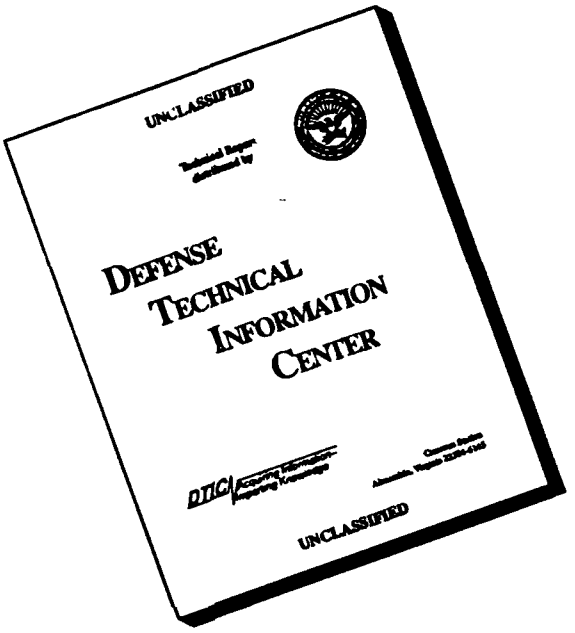

THIS DOCUMENT IS BEST QUALITY AVAILABLE. THE COPY FURNISHED TO DTIC CONTAINED A SIGNIFICANT NUMBER OF PAGES WHICH DO NOT REPRODUCE LEGIBLY.

REPORT DOCUMENTATION PAGE

1a. REPORT SECURITY CLASSIFICATION UNCLASSIFIED	1b. RESTRICTIVE MARKINGS
2a. SECURITY CLASSIFICATION AUTHORITY	3. DISTRIBUTION/AVAILABILITY OF REPORT Approved for public release; distribution is unlimited.
2b. DECLASSIFICATION/DOWNGRADING SCHEDULE	
4. PERFORMING ORGANIZATION REPORT NUMBER(S)	5. MONITORING ORGANIZATION REPORT NUMBER(S)
6a. NAME OF PERFORMING ORGANIZATION Naval Postgraduate School 6b. OFFICE SYMBOL (*If applicable*) 35	7a. NAME OF MONITORING ORGANIZATION Naval Postgraduate School
6c. ADDRESS (*City, State, and ZIP Code*) Monterey, CA 93943-5000	7b. ADDRESS (*City, State, and ZIP Code*) Monterey, CA 93943-5000
8a. NAME OF FUNDING/SPONSORING ORGANIZATION 8b. OFFICE SYMBOL (*If applicable*)	9. PROCUREMENT INSTRUMENT IDENTIFICATION NUMBER
8c. ADDRESS (*City, State, and ZIP Code*)	10. SOURCE OF FUNDING NUMBERS Program Element No. / Project No. / Task No. / Work Unit Accession Number

11. TITLE (*Include Security Classification*)
EVALUATION OF THE NAVAL RESEARCH LABORATORY LIMITED AREA DYNAMICAL WEATHER PREDICTION MODEL: TOPOGRAPHIC AND COASTAL INFLUENCES ALONG THE WEST COAST OF THE UNITED STATES

12. PERSONAL AUTHOR(S) Frank J. Grandau

13a. TYPE OF REPORT	13b. TIME COVERED	14. DATE OF REPORT (*year, month, day*)	15. PAGE COUNT
Master's Thesis	From To	March 1992	87

16. SUPPLEMENTARY NOTATION
The views expressed in this thesis are those of the author and do not reflect the official policy or position of the Department of Defense or the U.S. Government.

17. COSATI CODES			18. SUBJECT TERMS (*continue on reverse if necessary and identify by block number*)
FIELD	GROUP	SUBGROUP	mesoscale,numerical weather prediction,coastal circulation

19. ABSTRACT (*continue on reverse if necessary and identify by block number*)

This paper describes the evaluation of the NRL Limited Area Dynamical Weather Prediction Model in simulating coastal atmospheric mesoscale phenomena along the west coast of the United States during the period 0000 UTC 02 May - 1200 UTC 03 May 1990. A graphical comparison technique is used. Model output was compared horizontally with large-scale analyses, station data, cross-section analyses, and vertical profiles at specific locations. The model successfully simulated the wind and temperature fields, but failed to accurately replicate moisture and height fields

20. DISTRIBUTION/AVAILABILITY OF ABSTRACT	21. ABSTRACT SECURITY CLASSIFICATION	
[X] UNCLASSIFIED/UNLIMITED [ ] SAME AS REPORT [ ] DTIC USERS	UNCLASSIFIED	
22a. NAME OF RESPONSIBLE INDIVIDUAL Teddy R. HOLT	22b. TELEPHONE (*Include Area code*) 408-646-2861	22c. OFFICE SYMBOL MR/Ht

DD FORM 1473, 84 MAR — 83 APR edition may be used until exhausted. All other editions are obsolete.

Approved for public release; distribution is unlimited.

Evaluation of the Naval Research Laboratory Limited Area Dynamical Weather Prediction Model: Topographic and Coastal Influences Along the West Coast of the United States

by

Frank J. Grandau
Lieutenant Commander, United States Navy
B.S., Parks College of St. Louis University

Submitted in partial fulfillment
of the requirements for the degree of

MASTER OF SCIENCE IN METEOROLOGY AND PHYSICAL OCEANOGRAPHY

from the

NAVAL POSTGRADUATE SCHOOL
March 1992

Author: 
Frank J. Grandau

Approved by: 
T. R. Holt, Thesis Advisor


W.A. Nuss, Second Reader


Robert L. Haney, Chairman
Department of Meteorology

ABSTRACT

This paper describes the evaluation of the NRL Limited Area Dynamical Weather Prediction Model in simulating coastal atmospheric mesoscale phenomena along the west coast of the United States during the period 0000 UTC 02 May - 1200 UTC 03 May 1990. A graphical comparison technique was used. Model output was compared horizontally with large-scale analyses, station data, cross-section analyses, and vertical profiles at specific locations. The model successfully simulated the wind and temperature fields, but failed to accurately replicate moisture and height fields.

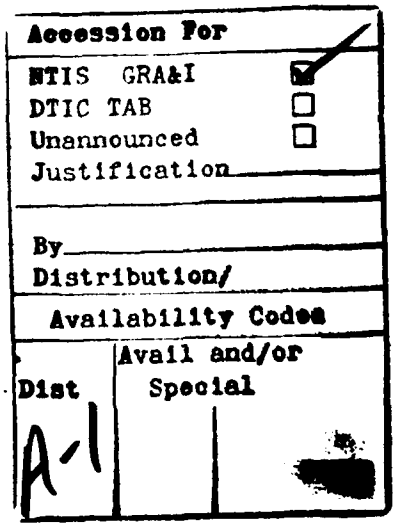

TABLE OF CONTENTS

ACKNOWLEDGEMENTS

I would like to extend my sincere thanks to Professor Teddy Holt for his guidance and support throughout the course of this study. His patience was truly remarkable. A special thanks goes to Professor Wendell Nuss for critical review of this thesis. Thanks also to Jim Cowie and Craig Motell for their programming assistance, and to Russ Schwanz and Donna Byrch of the Naval Postgraduate School's IDEA Lab who often came in during their off-hours and kept the IDEA Lab running; their support was instrumental in completing this work on time. Thanks to Dick Lind who provided the NPS profiler data. Special thanks to Chi-San Liou of NRL-Monterey for providing the initial model fields, and to Simon Chang of NRL for model development. Most important, however, thanks to Carolyn - my best friend and lifelong inspiration.

This research was funded by the NPS Direct Funded Merit Program. Technical sponsor was the NRL-Monterey.

I. INTRODUCTION

It has long been recognized that a large portion of significant weather occurs on the mesoscale (Orlanski 1975). The recent advent of large, fast computers has stimulated the development of limited area or regional numerical prediction models capable of capturing these mesoscale events. One such model, the Naval Research Laboratory (NRL) Limited Area Dynamical Weather Prediction Model, has developed continuously since its initial inception in the 1980's and is now used confidently to diagnose mesoscale phenomena and their interaction with larger scale systems (Holt et al. 1990; Schulz 1992). Although the NRL regional model has been run successfully for various geographic locations and domains throughout the world, it had yet to be used for the western United States area.

Within the western U.S. region, coastal and topographic interaction greatly influence the structure of the planetary boundary layer. Specific west coast topographic/coastal mesoscale studies include the Catalina Eddy event (Bosart 1983; Mass and Albright 1989) with its associated southerly surge (Dorman 1987) and windward damming of winds or frontal features in the Pacific Northwest (Mass and Ferber 1990).

Of all these studies, however, few prognostic modeling studies have been done. Ulrickson and Mass (1990) performed

numerical simulations of a Catalina Eddy using the three dimensional Colorado State University Mesoscale Model in order to investigate synoptic influences on pollutant transport in the Los Angeles Basin. Schultz and Warner (1982) and Glendening et al. (1986), using a two dimensional mixed layer model, also focused on the transports of pollutants in that basin. These studies were confined to the relatively small domain of the California bight and did not look beyond for greater spatial distribution of topographic and coastal influenced mesoscale events.

The purpose of this paper is to validate the ability of the NRL Limited Area Dynamical Weather Prediction Model to replicate atmospheric mesoscale features which occurred along the west coast of the United States during the period 0000 UTC 02 May 1990 to 1200 UTC 03 May 1990. The model had not been used previously to simulate sea/land breezes and mountain or valley winds comparable to those found in the California region, so no guidance was available concerning model performance or modifications required. Although several statistical techniques have been developed to quantitatively assess model results (Keyser and Anthes 1977; Willmott et al. 1985), a less rigorous technique of graphical and tabular comparison was used. This technique was chosen for several reasons. First, it allowed evaluation of predicted fields over the entire domain rather than at specific observation locations. Second, analysis fields (which might have served as observation

fields) were based on a synoptic observation network which could not completely resolve mesoscale phenomena. Any conclusions drawn from statistical comparison between analysis and forecast fields would therefore be confined to the larger scale.

In Chapter 2 of this paper the 3-D limited area model is described along with input data and topography fields used in the experiment. Chapter 3 describes observed synoptic and mesoscale features which occurred during the period 02-03 May 1990. The model's performance in handling large and mesoscale features is detailed in Chapter 4 and 5, respectively. Conclusions are included in the last chapter.

II. MODEL DESCRIPTION AND DATA SET

A. BASIC MODEL DESCRIPTION

The Naval Research Laboratory (NRL) Limited Area Dynamical Weather Prediction Model is a mesoscale, baroclinic, hydrostatic three dimensional model. Incorporating processes affecting both small and larger scale phenomena, it is appropriate for modeling the lower troposphere in which the balance of large-scale motions are approximately gradient. A brief description of the model is provided below; more extensive model descriptions are provided by Madala et al. (1987) and Chang et al. (1989).

The model's seven governing primitive equations are in surface pressure weighted flux form. Because of it's terrain following characteristics, sigma, defined as the ratio of pressure to surface pressure (Phillips 1957), is used as the vertical coordinate. Twenty three sigma levels resolve the vertical as indicated in Table 1. Five of the governing equations are prognostic. They include the u- and v- momentum equations, the thermodynamic equation, the moisture continuity equation, and the surface pressure tendency equation. The remaining two equations, the hydrostatic and continuity equations, are diagnostic. These equations form a closed system

Table I. Model Sigma Levels.

Model Level	Sigma	Del Sigma
1	0.05	0.1
2	0.15	0.1
3	0.25	0.1
4	0.35	0.1
5	0.45	0.1
6	0.55	0.1
7	0.64	0.08
8	0.715	0.07
9	0.78	0.06
10	0.835	0.05
11	0.88	0.04
12	0.915	0.03
13	0.94	0.02
14	0.957	0.014
15	0.969	0.010
16	0.978	0.008
17	0.985	0.006
18	0.99	0.004
19	0.9935	0.003
20	0.996	0.002
21	0.99775	0.0015
22	0.999	0.0010
23	0.99975	0.0005

for the seven dependent variables u, v, T, q, p_s, ϕ, and $d\sigma/dt$.

The equations are approximated by a first-order accurate finite difference scheme in space. This form enhances geostrophic adjustment while controlling small-scale gravity waves. A C-grid (Arakawa and Lamb, 1977) is used for the finite differencing. This grid best simulates geostrophic adjustment while conserving integral properties. The model has 103 X 91 horizontal grid points with uniform 1/6 degree resolution in latitude and longitude over the domain 28°-43°N, 130°-113°W. Temperature, geopotential, specific humidity and sigma are computed at mass points (i,j) while east-west velocity is computed at the midpoint of mass points along the x-axis and north-south velocity is computed at midpoints along the y-axis. Vertical velocity is evaluated at half-levels in the vertical between sigma surfaces.

Time integration utilizes a split-explicit scheme. This method allows a time interval equal to four times that of a conventional leapfrog scheme (Chang et al. 1989) by applying varying time steps for different modes of the linearized governing equations.

It is generally agreed that improper treatment at the boundaries of a regional model can offset any advantage gained by higher resolution. A temporal relaxation scheme is used in which the values within five grid lengths of the boundaries are relaxed toward the large-scale analysis. Boundary

conditions are updated every 12 hours and nudged towards hourly interpolations. This scheme is preferred over less capable fixed, time-dependent, or sponge schemes (Chang et al. 1989 and Holt et al. 1990).

Parameterized physics in the model include convective and nonconvective precipitation, dry convective adjustment and a parameterized planetary boundary layer.

A modified Kuo scheme (Kuo 1974) is used to parameterize convection precipitation. Convective precipitation occurs when grid scale low-level moisture convergence exists in a convectively unstable environment. This low-level moisture convergence either increases the humidity of the air or is condensed and precipitates as rain. Per Anthes (1977), the partitioning of latent heating and moistening is determined by the column mean relative humidity. Vertical distribution of heating is determined by the difference of temperature between the environment and the pseudoadiobat.

Nonconvective precipitation is reached when saturation occurs on the resolvable scale. The Clausius-Clapeyron equation is used to compute excess moisture and isobaric heating. Depending on the level at which saturation occurs, excess moisture either precipitates into the lower layers and evaporates or falls to the surface.

In order to neutralize superadiobatic lapse rates, dry convective adjustment parameterization is included in the model. The adjustment can take place over several layers

above the planetary boundary layer (PBL). This adjustment is activated when the static energy of a layer exceeds that of the adjacent higher layer. A slightly stable lapse rate results while total static energy is conserved.

PBL parameterization uses the turbulent kinetic energy (TKE) E - ϵ closure scheme (Gerber et al. 1989; Holt and Raman 1988). The surface boundary layer is parameterized by Monin-Obukov similarity (Businger et al. 1971). The large gradients in topography associated with the Sierra Nevada precluded the stable calculation of surface roughness length as a function of terrain heights; therefore, roughness lengths were assigned a constant value of 5 cm everywhere over land. This value is commonly used for most operational numerical weather prediction models. Over water, Charnock's relationship was used. In addition, the model incorporates a soil slab model (Blackadar, 1976) to predict ground temperature based upon the surface energy equation (Chang 1979). Initial sea surface temperatures (SST), however, were held constant in time throughout the model integration.

A second-order horizontal diffusion scheme is included in the model to suppress computational instability. The non-dimensional diffusion coefficient (approximately 0.004) is sufficiently small to enable the model to remain nearly undamped, but still prevent the growth of nonlinear instability in the solution. Horizontal diffusion of temperature and mixing ratio do not contain diffusion in the vertical,

rather, vertical diffusion occurs on terrain following sigma surfaces over mountainous topography.

B. INPUT DATA

The basic data set used in the initialization was the archived Fleet Numerical Oceanography Center's NOGAPS (Navy Operational Global Atmospheric Prediction System) 2.5 degree global analyses. Initial fields were sea level pressure (SLP), sea surface temperature (SST), D-values, u-components (U) and v-components (V) of velocity, temperature (T), and vapor pressure (e). These input fields are listed in Table 2. D-values were converted to geopotential heights using the NACA standard atmosphere relations (Haltiner and Martin, 1972).

Prior to initialization, NOGAPS fields were compared with the National Meteorological Center (NMC) final Global Data Assimilation System (GDAS) analysis. The only difference noted between the two analyses were in the moisture fields, particularly at lower levels. Although satellite imagery was not available, upper air data suggests that the GDAS moisture analyses may be more correct.

In order to initialize the model, fields were interpolated both horizontally and vertically. Horizontal interpolation was by cubic polynomial to 1/6 degree resolution. Bilinear interpolation was utilized along the boundaries. Fields were then vertically interpolated to the model's 23 sigma levels. Temperature was interpolated linearly in log pressure. Mixing

Table II. NOGAPS Gridded Input Fields.

Level (MB)	Parameters
Surface	SLP, SST
1000	D-Value, U, V, e, T
925	D-Value, U, V, e, T
850	D-Value, U, V, e, T
700	D-Value, U, V, e, T
500	D-Value, U, V, e, T
400	D-Value, U, V, e, T
300	D-Value, U, V, e, T
250	D-Value, U, V, T
200	D-Value, U, V, T
150	D-Value, U, V, T
100	D-Value, U, V, T
70	D-Value, U, V, T
50	D-Value, U, V, T
30	D-Value, U, V, T
20	D-Value, U, V, T
10	D-Value, U, V, T

ratio was interpolated exponentially in pressure. U and V velocity components were interpolated linearly in pressure.

Topography was derived from the U.S. Navy global 10-minute elevation data. Five point horizontally-averaged smoothing was applied to the elevation data. This provided a near-realistic terrain field for the model validation run. Figures 1 and 2 show domain wide and hi-resolution California coastal terrain fields, respectively.

ratio was interpolated exponentially in pressure. U and V velocity components were interpolated linearly in pressure.

Topography was derived from the U.S. Navy global 10-minute elevation data. Five point horizontally-averaged smoothing was applied to the elevation data. This provided a near-realistic terrain field for the model validation run. Figure 1 shows the validation terrain field.

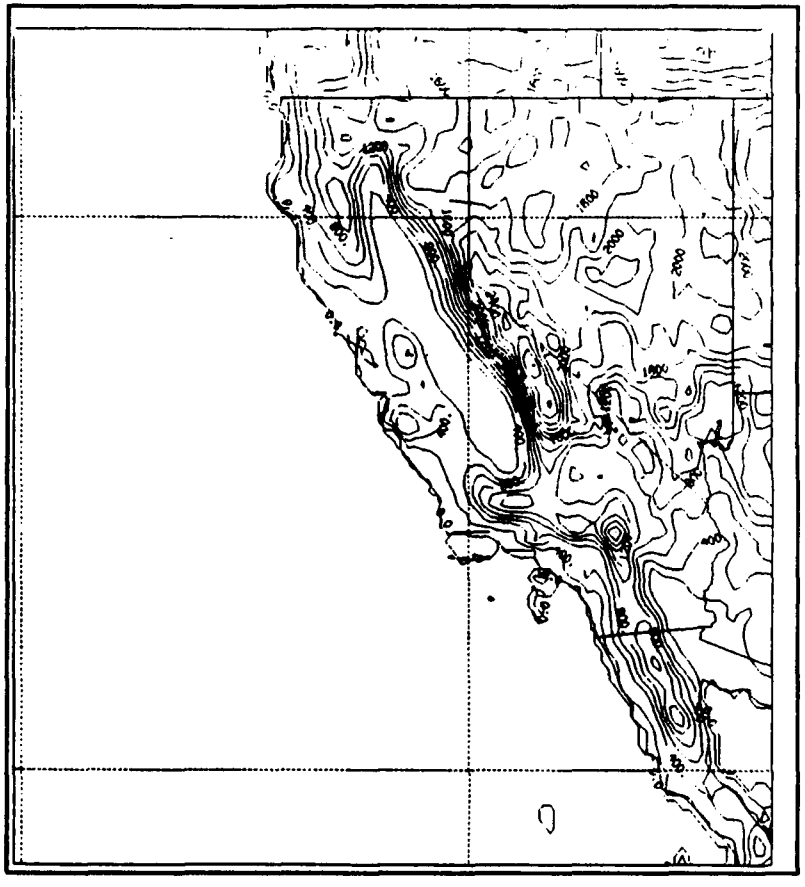

Figure 1. Terrain field (m).

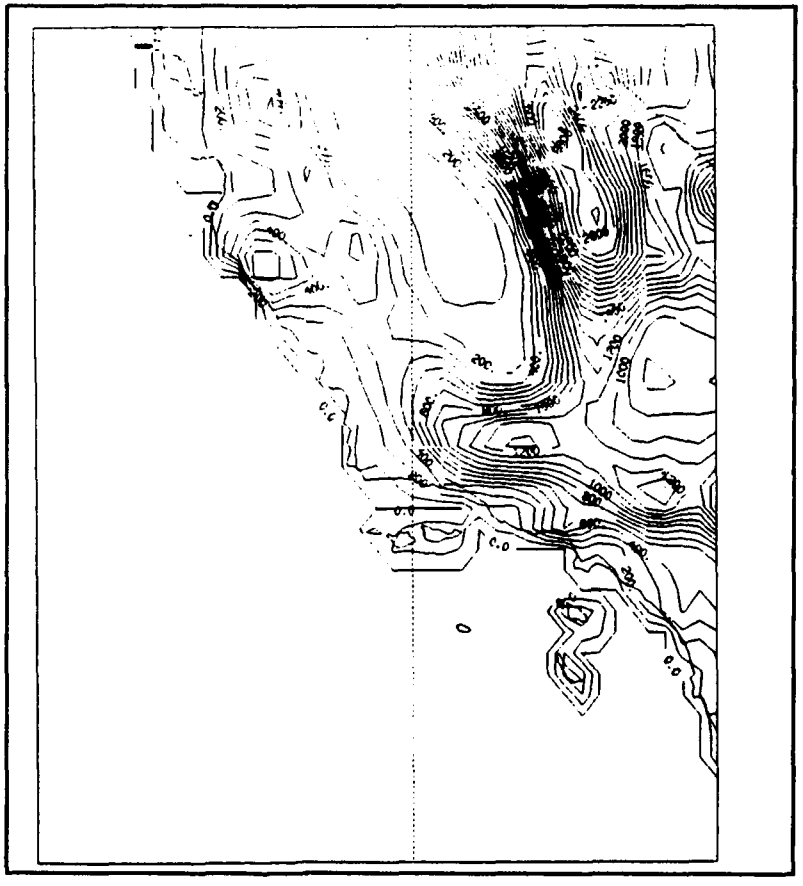

Figure 2. Coastal terrain field (m).

III. METEOROLOGICAL SITUATION (02-03 MAY 1990)

A. SYNOPTIC SCALE ANALYSIS

Figures 4, 6, 8, and 10 show 12-hour 2.5° resolution FNOC NOGAPS 500 mb height and temperature analyses for the period 0000 UTC 02 May 1990 to 1200 UTC 03 May 1990. After initial weakening during the first 12 hours, a high amplitude pressure ridge at 500 mb in the central East Pacific was slowly building northeast through the period (Figure 6). Subsiding northerly flow on the east side of the ridge created strong low-level and surface-based inversions along the entire California coast. A low pressure cell over western Arizona was stationary during the first 12 hours of the period and deepened slightly (Figure 4). During the final 24 hours (Figures 8 and 10), however, this low filled and eventually moved off to the east-northeast. A thermal trough over the Pacific Northwest at 0000 UTC 02 May (Figure 4) moved south to near southern California by 1200 UTC 03 May (Figure 10). This troughing was indicative of a short wave, with its associated positive vorticity, in the flow pattern aloft.

Figures 3, 5, 7, and 9 show 12-hour 2.5° resolution FNOC NOGAPS sea level pressure analyses for the period 0000 UTC 02 May 1990 to 1200 UTC 03 May 1990. A high pressure cell, initially located in the central East Pacific (Figure 3), had

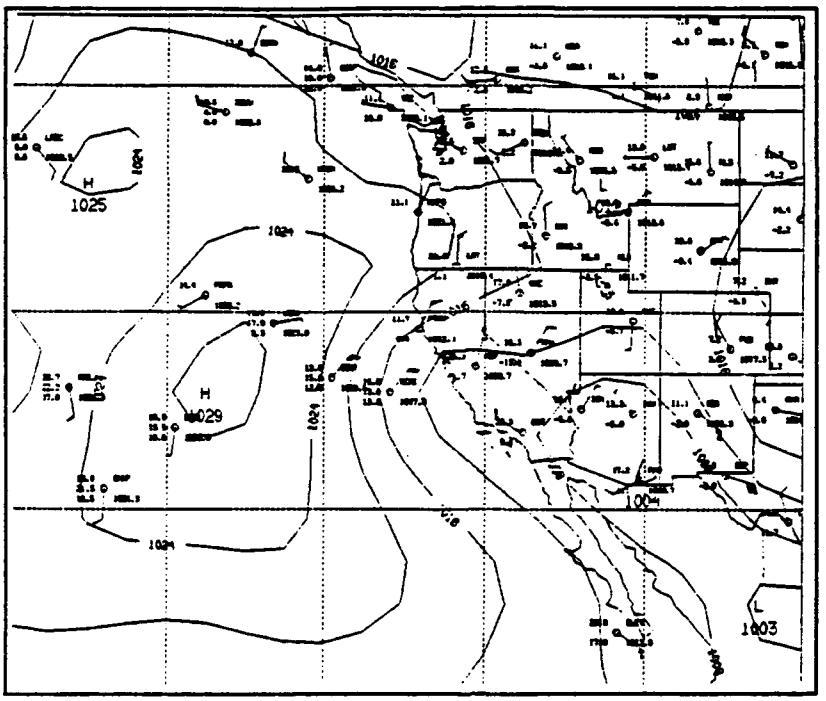

Figure 3. 0000 UTC 02 May 1990 NOGAPS Sea Level Pressure (mb) Analysis.

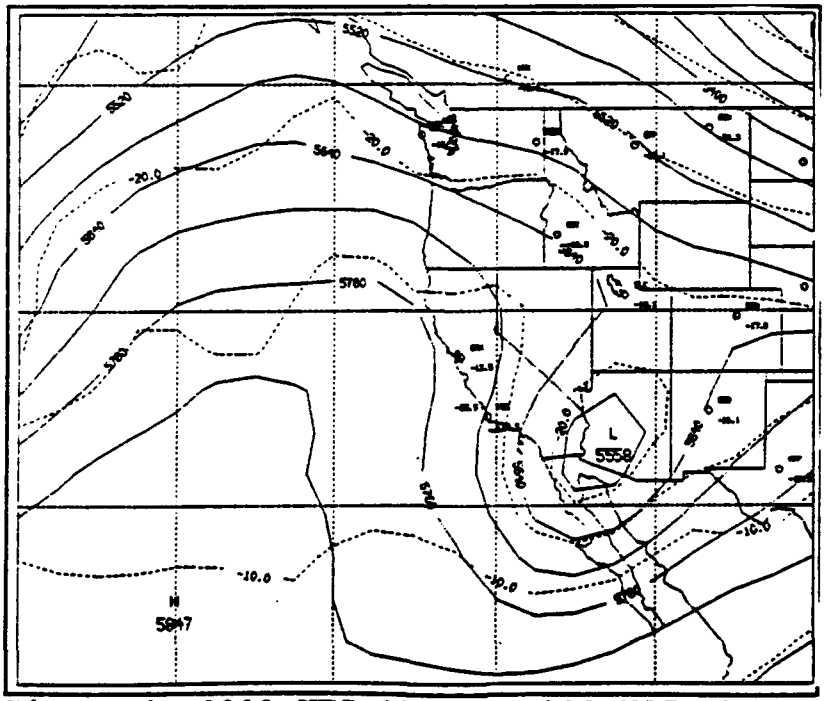

Figure 4. 0000 UTC 02 May 1990 NOGAPS 500 mb analysis. Heights (m, solid) and temperature (°C, dashed).

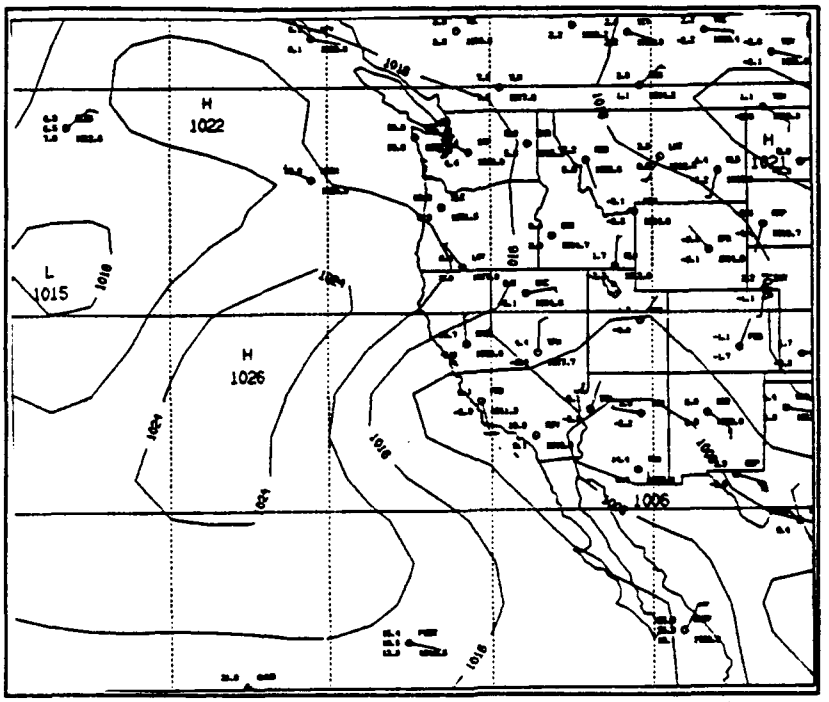

Figure 5. 1200 UTC 02 May 1990 NOGAPS Sea Level Pressure (mb) Analysis.

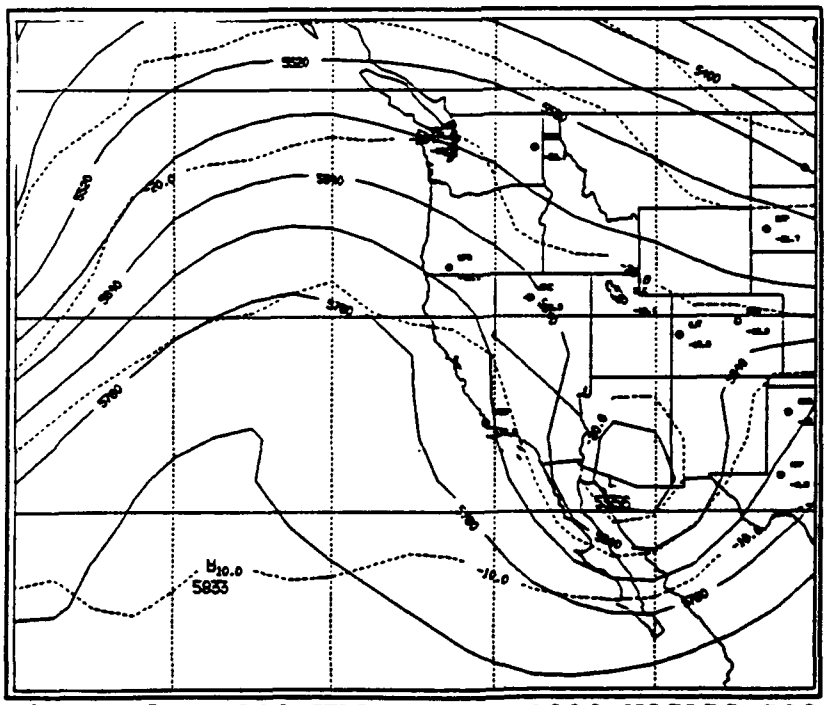

Figure 6. 1200 UTC 02 May 1990 NOGAPS 500 mb analysis. Heights (m, solid) and temperature (°C, dashed).

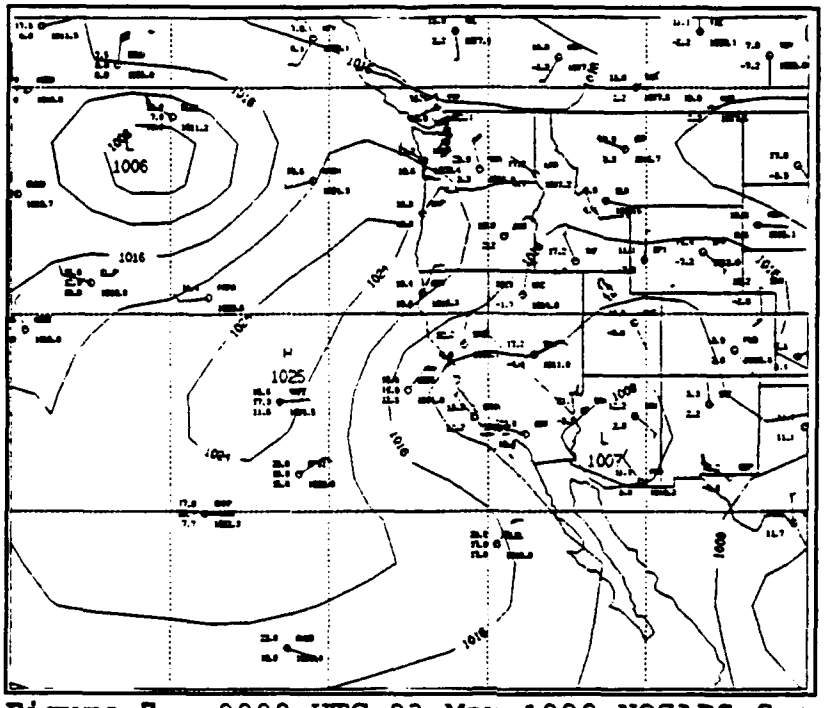

Figure 7. 0000 UTC 03 May 1990 NOGAPS Sea Level Pressure (mb) Analysis.

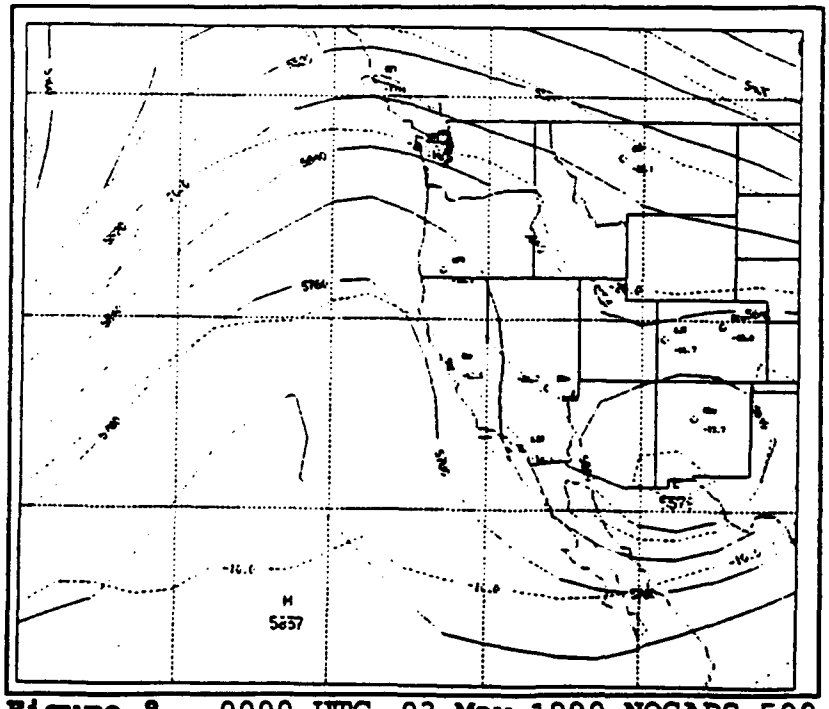

Figure 8. 0000 UTC 03 May 1990 NOGAPS 500 mb analysis. Heights (m, solid) and temperature (°C, dashed).

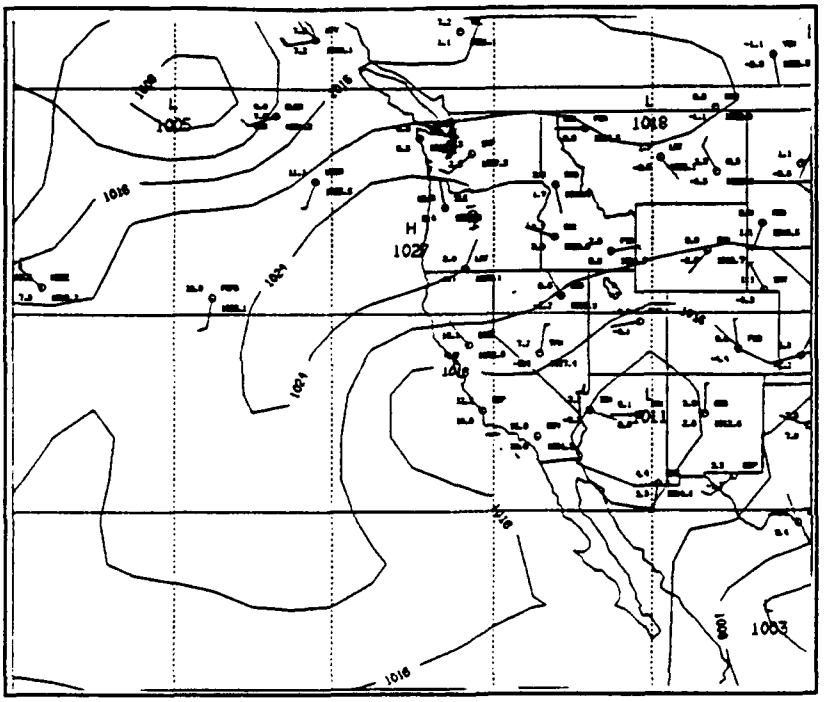

Figure 9. 1200 UTC 03 May 1990 NOGAPS Sea Level Pressure (mb) Analysis.

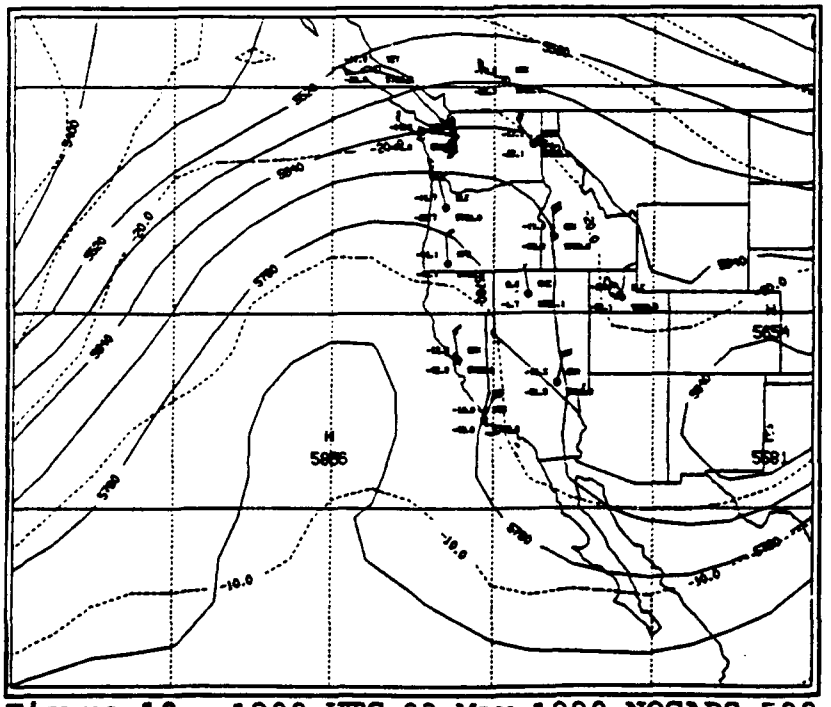

Figure 10. 1200 UTC 03 May 1990 NOGAPS 500 mb analysis. Heights (m, solid) and temperature (°C, dashed).

intensified and moved to near the Oregon coast by 1200 UTC 03 May (Figure 9). A low pressure system, situated in southern Arizona, had moved slowly north and filled through out the period. Thermal troughing in central California was initially coupled to this surface low, but by 1200 UTC 03 May (Figure 9) had moved offshore.

B. MESOSCALE ANALYSES

Several mesoscale atmospheric phenomena have been observed and studied during the period, 0000 UTC 02 May -1200 UTC 03 May. All three were coastal and possibly topographically induced and are therefore relevant to this paper.

Streed (1990) successfully observed land/sea breeze structure for the period 02-03 May 1990 using the UHF doppler wind profiler at the Naval Postgraduate School, Monterery, CA. Although it is impossible to determine the horizontal extent of the land-sea breeze from a single observation point, vertical structure and intensity were determined. Specifically, the land-sea breeze was confined to the lowest 2500 meters of the atmosphere. Although the return limb of the flow aloft is not well defined for either the land or sea breeze components, the lower limb is easily discerned in the data (Figure 11) to be confined to the lowest 1000 meters. From 0400 UTC 02 May 1990 to 2000 UTC 02 May 1990, the land/valley breeze sets up from the south, aligned with the topography of the

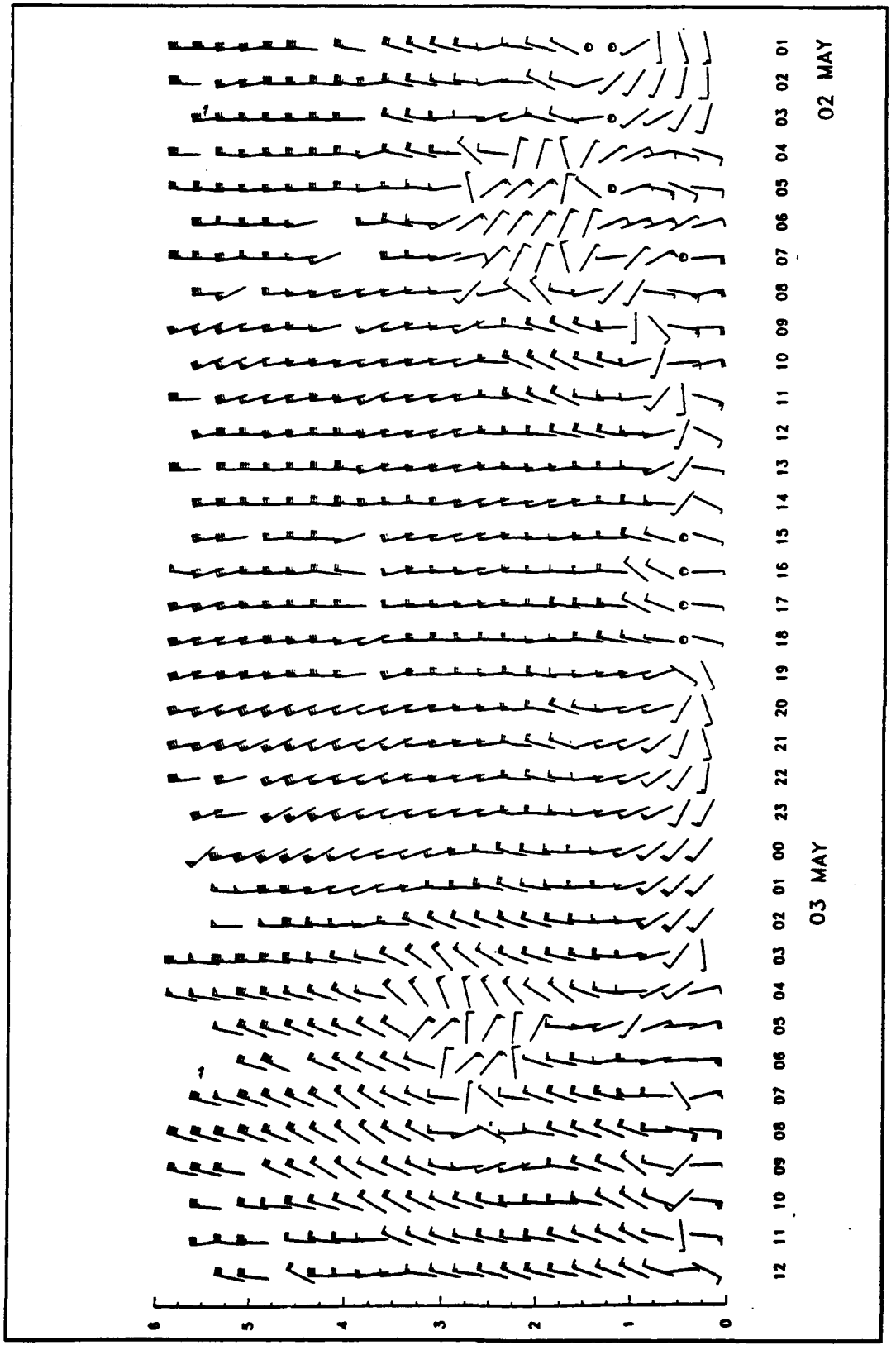

Figure 11. Time/Height (km) Profile of Winds from NPS Fort Ord Profiler Site (0000 UTC 02 May 1990 - 1200 UTC 03 May 1990).

Salinas River valley. The sea breeze persisted from approximately 2100 UTC 02 May 1990 to 0300 UTC 03 May 1990.

In his case study of a stratus/fog event, Corkill (1991) describes mesoscale features affecting the California region during the period 0000 UTC 02 May 1990 to 1200 UTC 03 May 1990. Surface mesoscale analyses were made using a multiquadric interpolation scheme (Hardy 1990). The sea level pressure analysis for 0000 UTC 02 May 1990 (Figure 12) shows a complex low pressure pattern in central California associated with the thermal trough. Offshore, flow is from the north with no mesoscale structure evident. By 1200 UTC 03 May, the sea level pressure analysis (Figure 13) shows a mesoscale trough had developed offshore central California and was responsible for southerly flow along the coast. This situation is similar to those depicted in the Mass and Albright (1987) case studies of topographically trapped alongshore surge along the west coast of North America. This analysis is very different from the NOGAPS analysis (Figure 9).

A third mesoscale feature, the Catalina Eddy, is discernable in the surface and upper air data (see Chapter 5). In particular, soundings at San Clemente (NSI), El Toro (LIO), and Point Mugu (NTD) suggest a closed Eddy vortex at both 1200 UTC 02 May 1990 and at 1200 UTC 03 May 1990. This feature is coupled to the southerly surge phenomena. Mass and Albright (1989) describe the synoptic pattern favorable for formation of a Catalina Eddy. The Catalina Eddy results from the

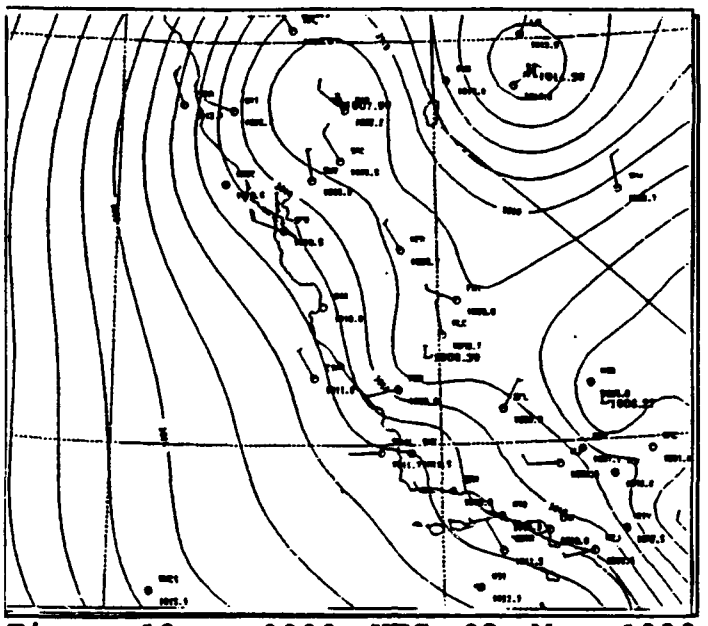

Figure 12. 0000 UTC 02 May 1990 Mesoscale SLP (mb) Anal (Corkill, 1991).

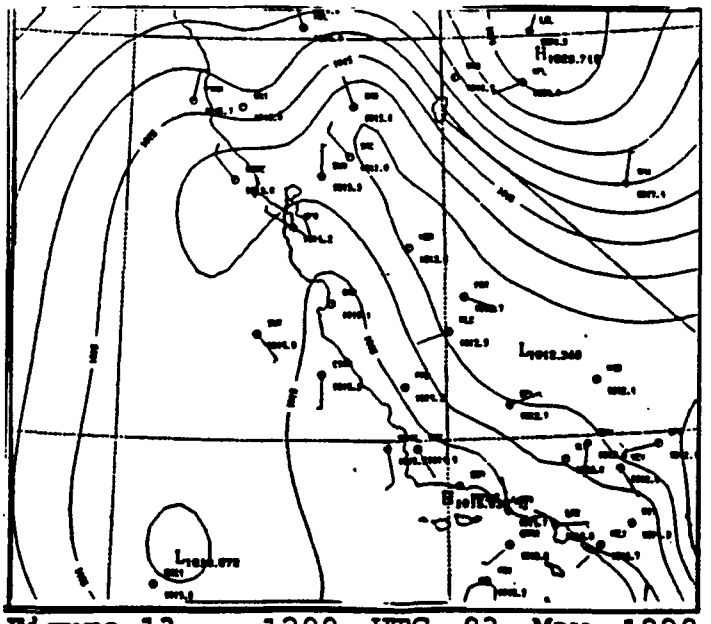

Figure 13. 1200 UTC 03 May 1990 Mesoscale SLP (mb) Anal (Corkill, 1991).

interaction of synoptic scale flow with the formidable topographic barriers of the region. The first process in the development of the Eddy is the passage of a short-wave trough into the Pacific Northwest (Figure 6). A pre-existing 850 mb trough in the western United States extends southwestward towards the southern California bight, while at the surface the interior heat trough extends northwestward into central California (Figure 5). These synoptic features intensify the lower tropospheric pressure gradient along the central California coast, and strengthen the northerly flow in the region.

With a strengthening northerly flow approaching the San Ynez Mountains to the north of the bight, synoptic and mesoscale lee troughing become evident within the bight. This troughing produces an alongshore pressure gradient with lower pressure to the north. As a result, ageostrophic southerly flow develops within approximately a Rossby radius (approximately 100 km) of the coastal mountain barrier. With relatively geostrophic northerlies remaining further offshore, considerable cyclonic vorticity is created in the coastal zone.

As the southerly flow increases, there is an increase in the depth of the cool, moist marine layer in the coastal zone, resulting in a narrow coastal pressure ridge. As the coastal pressure ridge intensifies and extends northward, an isolated low center offshore often becomes evident.

Catalina Eddy events continue as long as the synoptic-scale conditions support the required alongshore pressure gradient. As the synoptic pattern evolves and the inland troughing attenuates, the northerly flow to the west and north of Point Conception weakens, the alongshore pressure gradient reverses, and the normal winds in the bight are reestablished.

IV. MODEL PERFORMANCE FOR SYNOPTIC SCALE PHENOMENA

A. GENERAL

The model was evaluated for 36 hours of integration during the period 0000 UTC 02 May to 1200 UTC 03 May. This particular time period was chosen for a variety of reasons. Not only was the Naval Postgraduate School (NPS) wind profiler operating during this period, but the research vessel PT SUR was offshore in Monterey Bay providing upper air soundings every six hours commencing at 1800 UTC 02 May. Thus, in addition to routine NWS surface and upper air reports, two other vertical high resolution data sets were available.

The synoptic situation was also considered when choosing the integration period. The synoptic pattern was variable enough during the period to provide for both alongshore and low level off land flow over the central California coast. Additionally, it was responsible for generating significant topographic and coastal induced mesoscale systems (see previous chapter).

The evaluation was concerned with the model's performance in predicting primarily geopotential height, temperature, and wind fields and, secondarily, moisture fields. Model output at 12, 24, and 36 hour integrations were examined. Three comparison schemes were utilized. First, model output was

compared with the large scale interpolated NOGAPS analyses (with corresponding station plots) at the surface and 850 mb, 700 mb, and 500 mb constant pressure levels. Second, cross-section analyses were examined. Third, vertical profile comparisons were made at upper air sounding locations.

Both model output and interpolated NOGAPS fields were plotted using the NPS Interactive Digital Environmental Analysis (IDEA) Lab GENAL general analysis package. IDEA Lab GEMPAK routines were utilized to plot vertical profiles and perform model independent cross-section analysis. The GEMPAK cross-section analysis scheme is based upon cubic spline interpolation of sounding data. This analysis scheme is limited in its ability to resolve small scale features, and its interpolation scheme often generates fictious mesoscale structure, particularly in the higher elevations. For these reasons, it's primary use was to verify the model's handling of large scale processes.

The GEMPAK cross-section analysis is done on a straight line between the first and last stations; the positions of intervening stations are proportional to the perpendicular projections of the actual positions onto the section line. Since at least four stations are required for the scheme, four of the section lines were extended beyond the model domain. Figure 14 shows the section lines; because of data nonavail-ability, not all section lines were used at each evaluation time. Orientation of the sections are based on sounding

station alignment rather than concern with examining a specific atmospheric phenomena.

Input fields at 0000 UTC 02 May and output fields at 1200 UTC 02 May are discussed below in detail. Supporting charts are included for these times in order to illustrate the validation process. The same validation process was applied to the remaining two times, 0000 and 1200 UTC 03 May; however, only a summary and any significant departures during these periods from previously discussed model performance is included.

B. ANALYSIS AT 0000 UTC 02 MAY 1990 (MODEL INPUT FIELDS)

In order to determine the fidelity of the initial large-scale analysis, comparison is made of the 0000 UTC 02 May 1990 interpolated NOGAPS fields (which serve as the model initialization fields) to observations and GEMPAK cross-section analyses.

1. Constant Pressure Surfaces

a. Surface

The vertical interpolation scheme uses an algorithm which extrapolates temperature from the fifth lowest sigma level downward to obtain surface pressure. This leads to disparity between interpolated surface pressure fields and the large-scale NOGAPS sea level pressure pattern. In general, however, the interpolated NOGAPS sea level pressure pattern appears reasonable (Figure 15). A single ship report (XCM1)

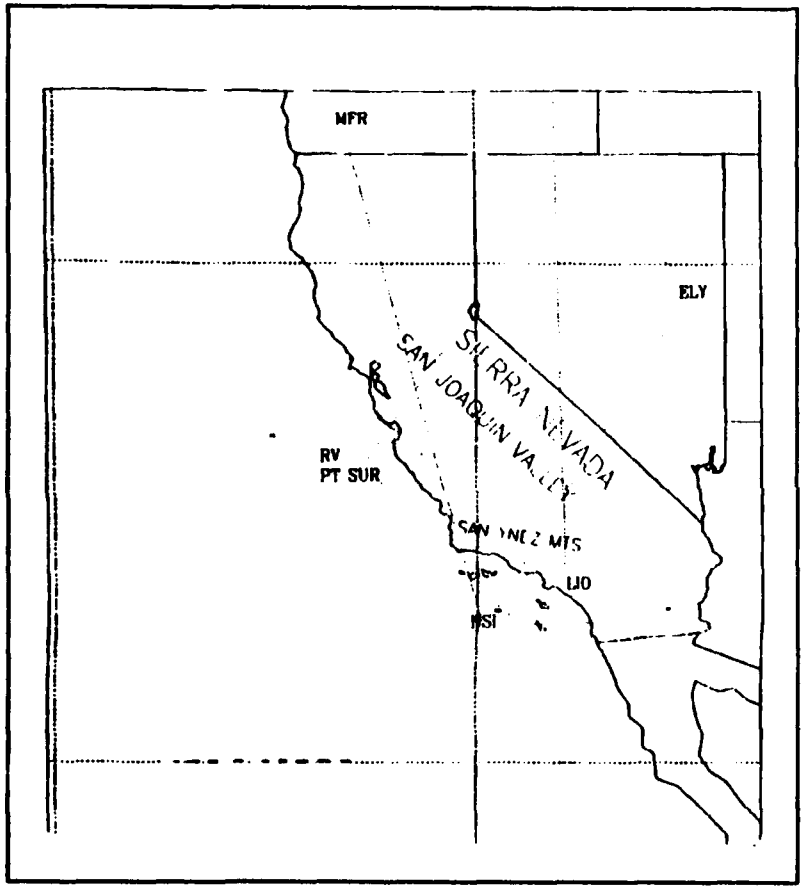

Figure 14. Validation cross-sections (dashed).

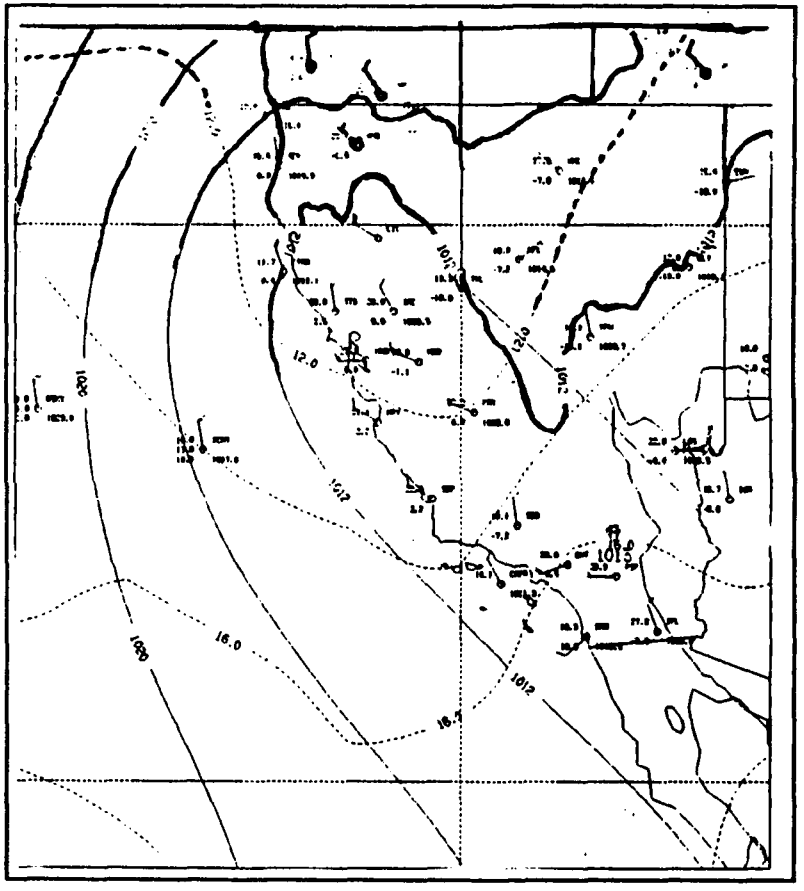

Figure 15. 0000 UTC 02 May 1990 Initial Sea Level Pressure (mb) and Temperature (°C) Analysis.

suggests slightly weaker pressure gradients offshore than analyzed. The interpolation has produced slightly stronger ridging over the mountains than indicated on the synoptic scale analysis (Figure 3). Thermal troughing over central California appears reasonable in orientation and magnitude. West and southwest winds at several coastal stations in central and southern California suggest a more complex mesoscale structure exists than indicated by the interpolated analysis. Sea surface temperatures look reasonable based on climatology and generally reflect the expected pattern for a cold southward flowing California current.

b. 850 Mb Constant Pressure

The 850 mb height and temperature analysis (Figure 16) does not deviate significantly from the synoptic scale analysis (not shown). Gaps in the contours indicate where the 850 mb pressure level intersects topography; no extrapolated analysis below the terrain was done within that region. Weak thermal ridging with associated warm air advection exists offshore of central California; observations support this thermal analysis. The initial wind field, shown in Figure 17 by a wind vector at every other point of the model grid, departs significantly from observed winds, particularly at Winnemuca (WMC), Medford (MFR) and Desert Rock (DRA). These initial wind field deviations most likely reflect observed topographic effects.

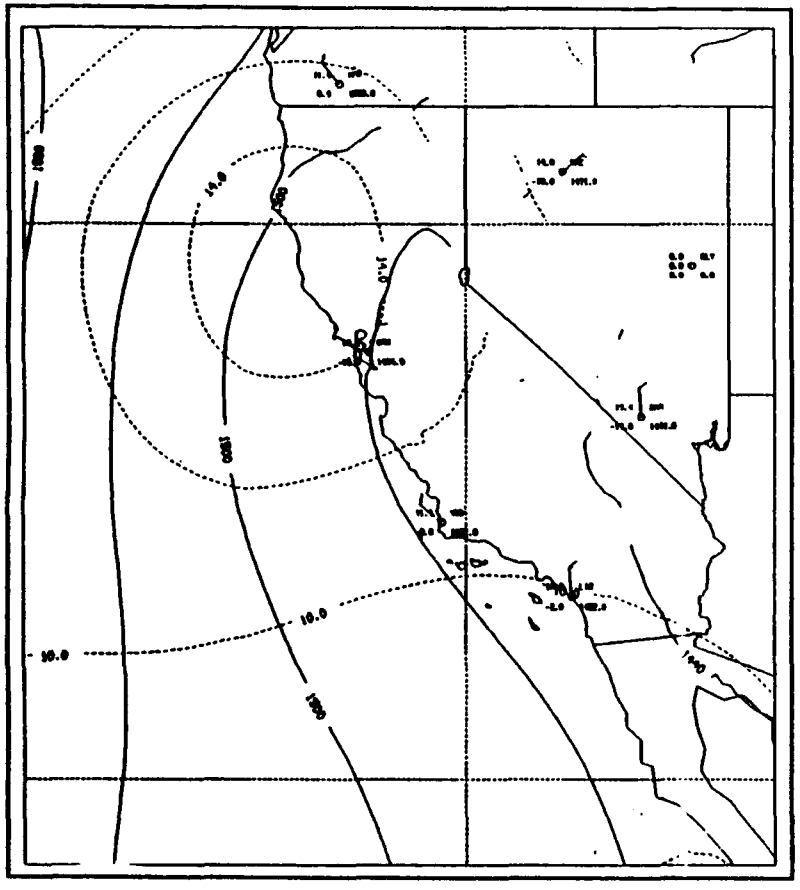

Figure 16. 0000 UTC 02 May 1990 Initial 850 mb Height (m) and Temperature (°C) Analysis.

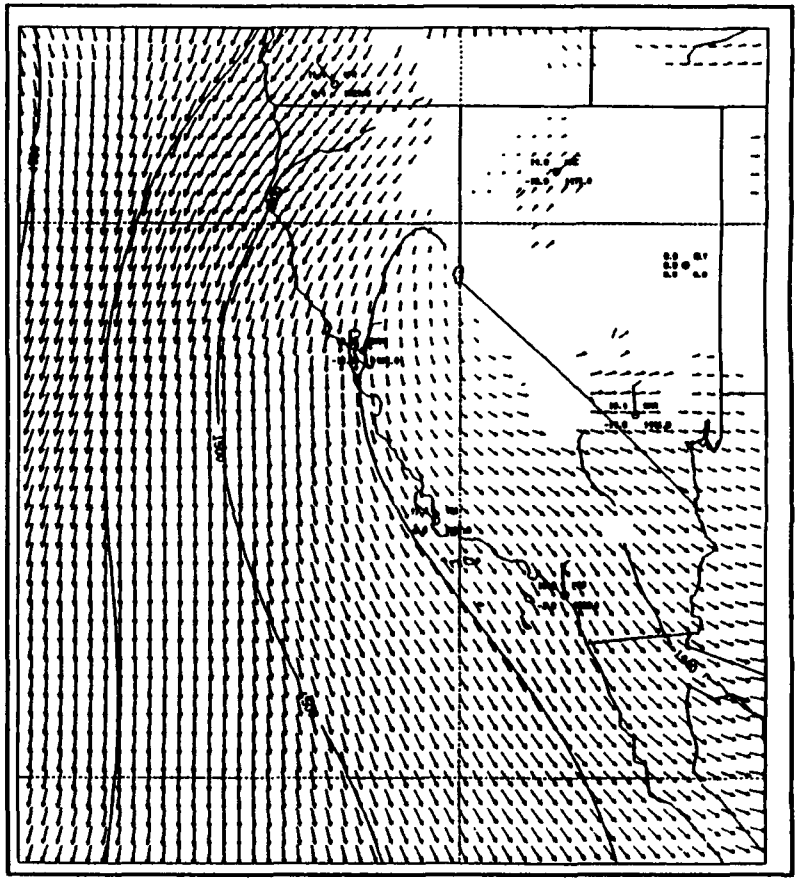

Figure 17. 0000 UTC 02 May 1990 Initial 850 mb Wind and Height (m) Field.

The mixing ratio analysis at 850 mb shows considerable dry air off the northern and central California coast. A moisture maximum exists over western Nevada east of the Sierra Nevada. Examination of lower level moisture fields show this maximum tilts eastward and weakens with height. As previously mentioned, there is a significant departure between the NOGAPS and NMC GDAS moisture analyses. This difference is most notable at 850 mb where NOGAPS and GDAS moisture analyses appear almost 180 degrees out of phase. Sounding data and cross-section analysis suggest that the NMC scheme may be more correct in handling moisture.

c. 700 Mb Constant Pressure

The 700 mb pressure surface lies just above the highest terrain of the Sierra Nevada. At this level, the atmosphere is nearly geostrophic. Wind, height, and thermal observations should therefore be consistent with the initial analysis fields. The height and temperature analysis (figures not shown) shows only minimal noise over the mountains. This noise is an artifact of the vertical interpolation scheme and reflects extrapolation of the temperature field below the lowest sigma level to the surface. The noise is most pronounced at low-levels and over mountainous terrain. The height field and sounding data correlate well at all locations. The thermal pattern generally reflect the observations. There is some problem, however, in positioning

specific temperature contours, most notably in the weak thermal gradient over Nevada. Wind field and observations are in fair agreement everywhere but at WMC. The moisture analysis shows the western Nevada maximum as well as increasing the moisture to the northwest. Drier air lies off the central and southern California coasts. Considerably greater agreement exists between the NOGAPS and GDAS moisture fields at this level than at 850 mb and below.

d. 500 Mb Constant Pressure

At 500 mb, terrain influences are non-existent. Height, thermal, (Figure 18) and wind fields (Figure 19) are in good agreement with observed data. Because of the low moisture content in the atmosphere at these levels, the moisture field was not verified.

2. CROSS-SECTION ANALYSES

Cross-section analyses along the Medford (MFR) to San Nicholas Island (NSI) transect (see Figure 14) were made for both the interpolated analysis fields (using GENAL) and upper air sounding data (using GEMPAK). As expected, no BL structure is evident in the interpolated fields. Potential temperature cross-sections (Figures 20 and 21) at 0000 UTC 02 May 1990 agree on general patterns, although the GEMPAK analysis does suggest some BL structure south of Oakland. Considering the time of day (late afternoon), BL instability is expected.

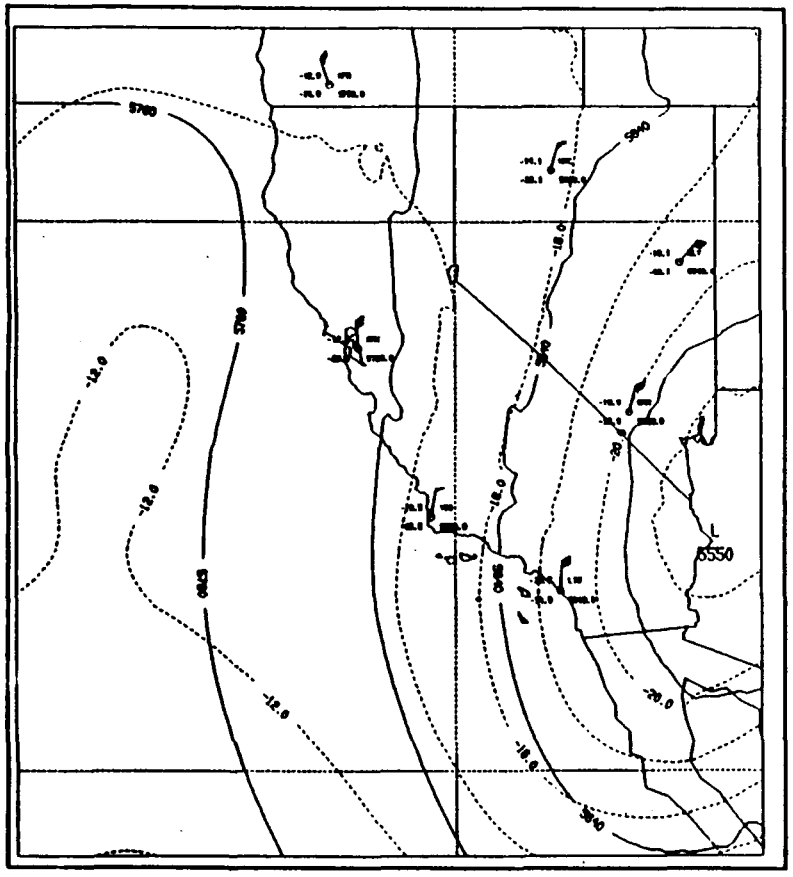

Figure 18. 0000 UTC 02 May 1990 Initial 500 mb Height (m) and Temperature (°C) Analysis.

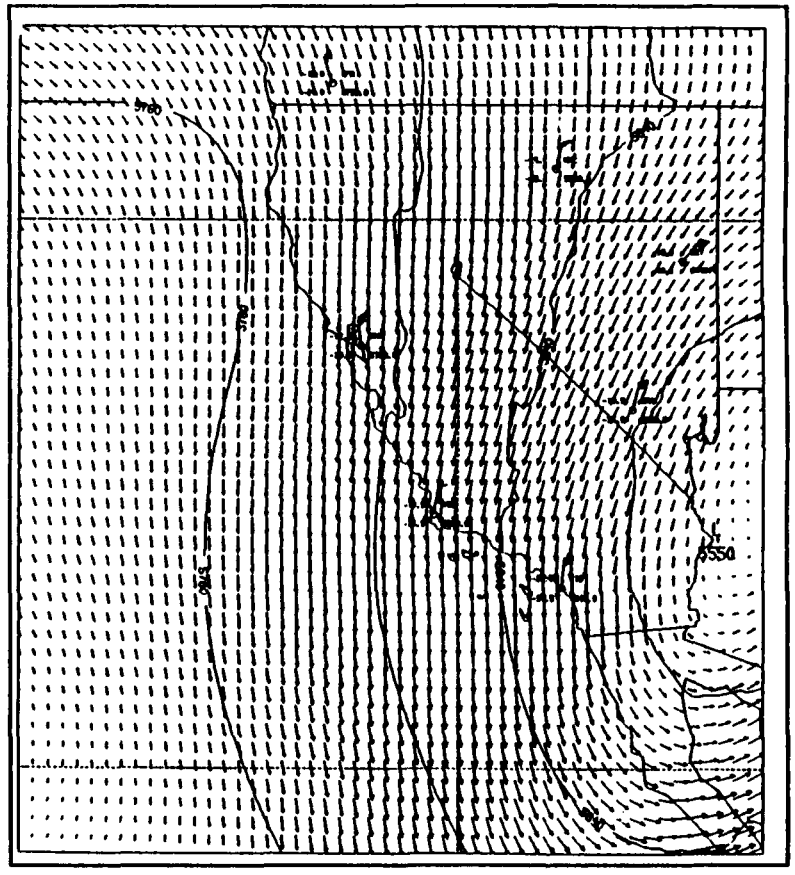

Figure 19. 0000 UTC 02 May 1990 Initial 500 mb Wind and Height (m) Field.

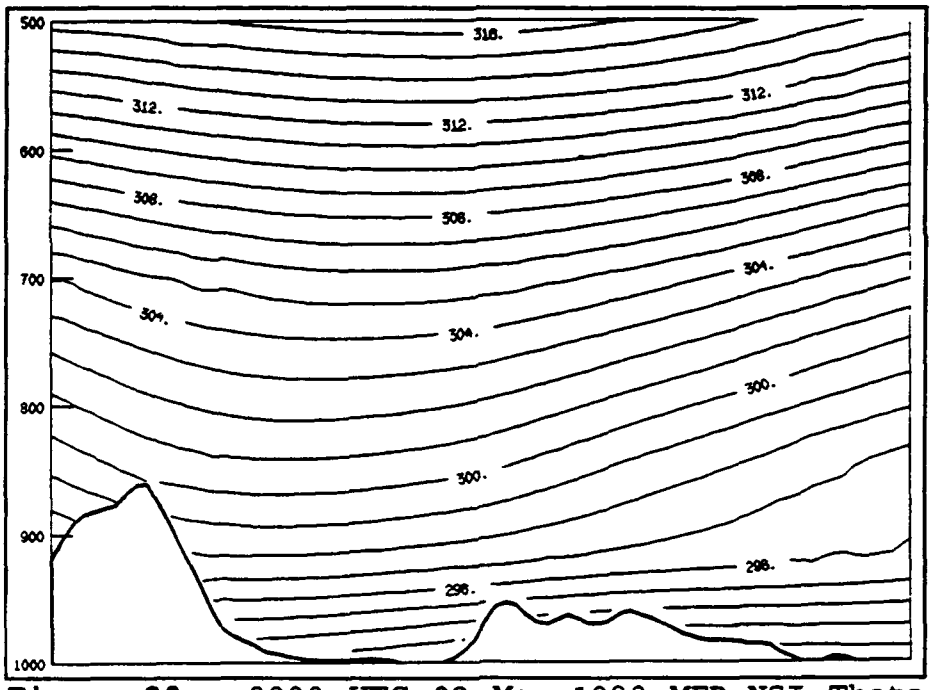

Figure 20. 0000 UTC 02 May 1990 MFR-NSI Theta (°K) Model Input Cross-section Analysis.

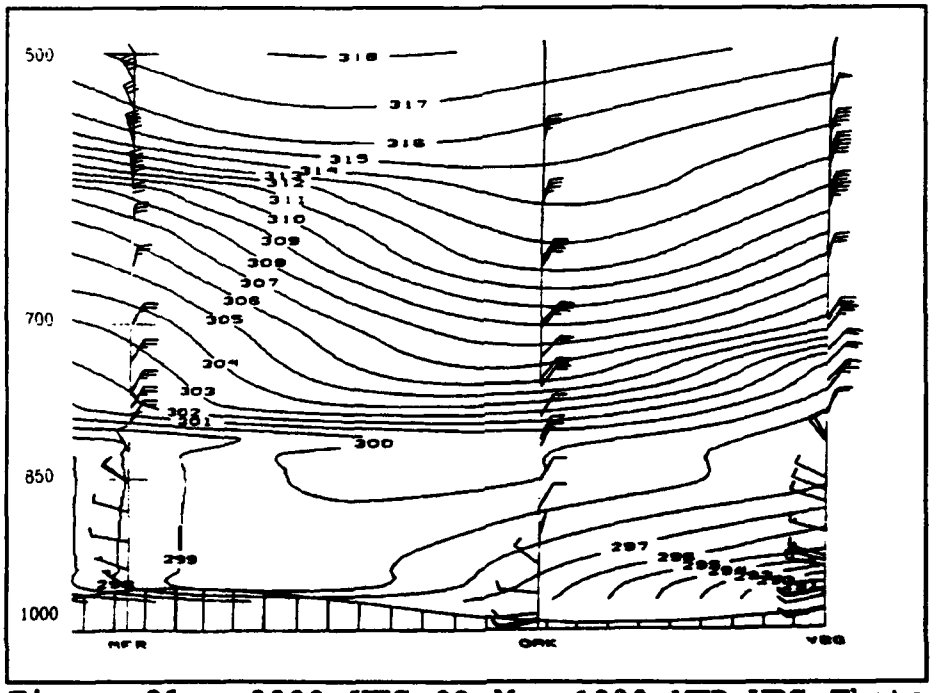

Figure 21. 0000 UTC 02 May 1990 MFR-VBG Theta (°K) GEMPAK Cross-section Analysis.

Mixing ratio cross-sections (Figures 22 and 23) disagree significantly, particularly south of OAK. The GEMPAK analysis shows considerably drier air above 900 mb, suggesting that the model input data may be too moist in this region. The NMC GDAS moisture analysis lends support to this conclusion.

Both the u-velocity cross-sections (Figures 24 and 25) and v-velocity cross-sections (Figures 26 and 27) above approximately 800 mb agree well, but show some disparity at lower levels. Most notably, the lower GEMPAK v-component velocities in the vicinity of MFR reflect topographic influences not discerned in the interpolated field analysis. Also, a southerly wind component near Vandenberg AFB (VBG) is not analyzed in the interpolated fields.

C. MODEL OUTPUT AT 1200Z 02 MAY 1990

In order to determine the model's ability to successfully forecast large-scale synoptic features, comparison is now made of the 12 hour model simulation at 1200 UTC 02 May 1990 to the corresponding interpolated analyses, observations, and GEMPAK cross-section analyses.

1. Constant Pressure Surfaces

a. Surface

The model's forecast surface pressure and temperature fields (Figure 28) differs significantly from the interpolated analysis (Figure 29). Most notably, the model depicts a large region of broad scale lower pressure off the

Figure 22. 0000 UTC 02 May 1990 MFR-NSI Mixing Ratio (g/kg) Model Input Cross-section Analysis.

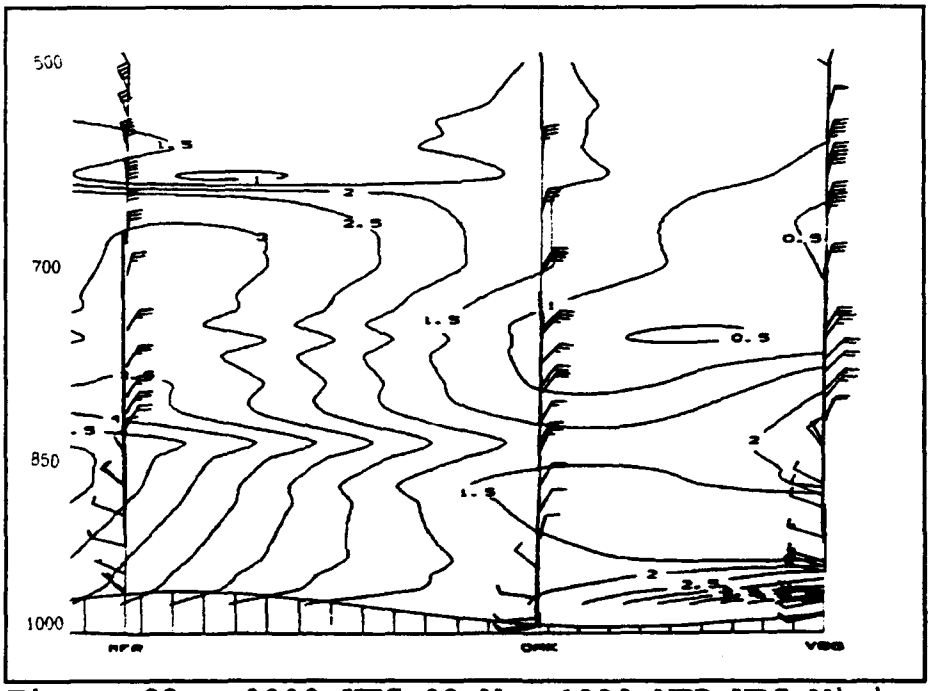

Figure 23. 0000 UTC 02 May 1990 MFR-VBG Mixing Ratio (g/kg) Model Input Cross-section Analysis.

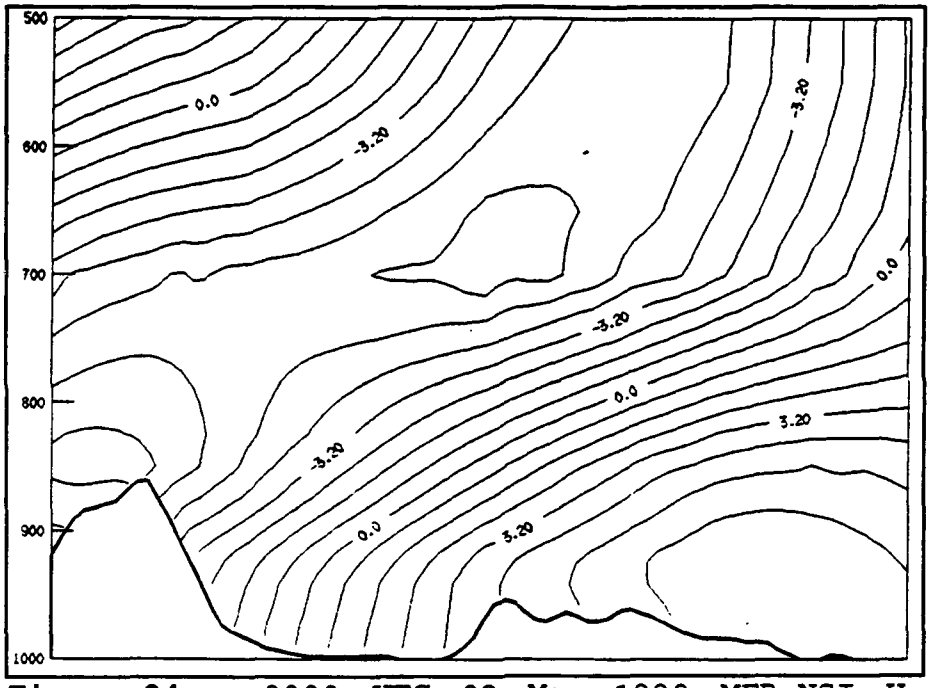

Figure 24. 0000 UTC 02 May 1990 MFR-NSI U-velocity Model Input Cross-section Analysis. Eastward (m/s, solid). Westward (m/s, dashed).

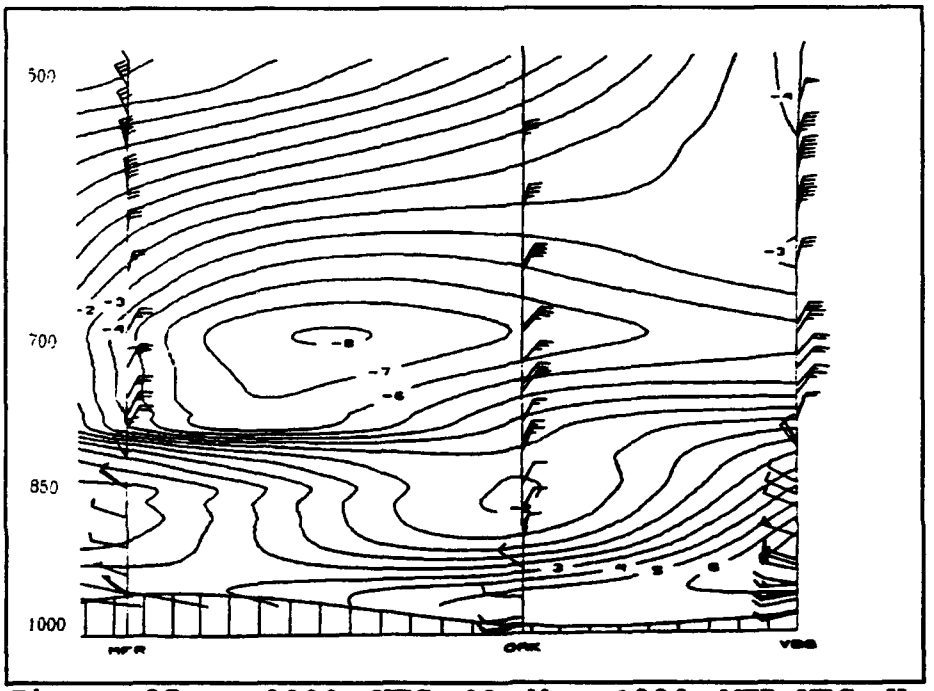

Figure 25. 0000 UTC 02 May 1990 MFR-VBG U-velocity Model Input Cross-section Analysis. Eastward (m/s, solid). Westward (m/s, dashed).

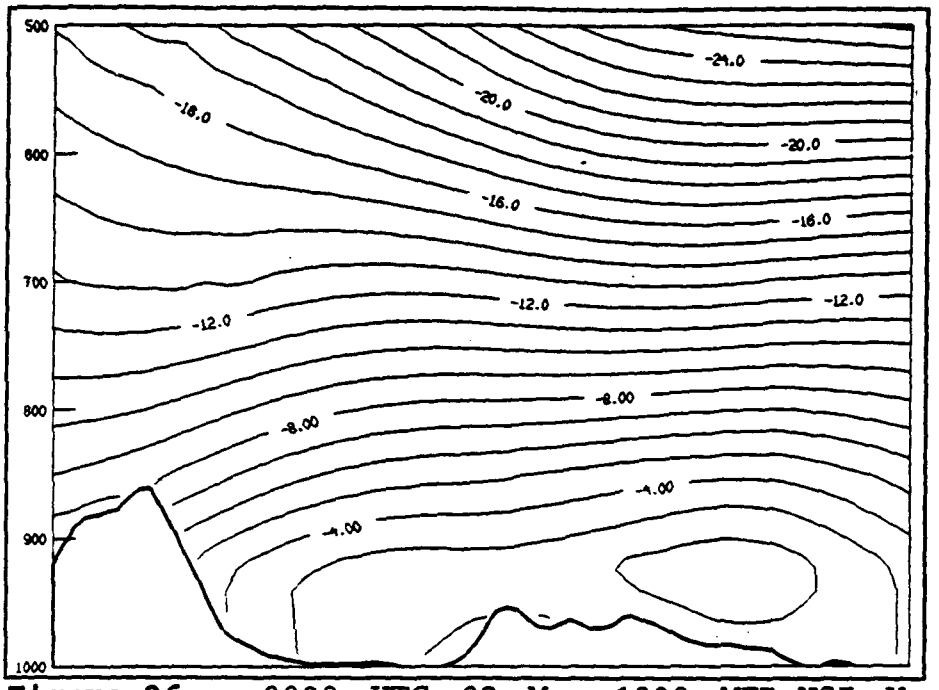

Figure 26. 0000 UTC 02 May 1990 MFR-NSI V-velocity Model Input Cross-section Analysis. Northward (m/s, solid). Southward (m/s, dashed).

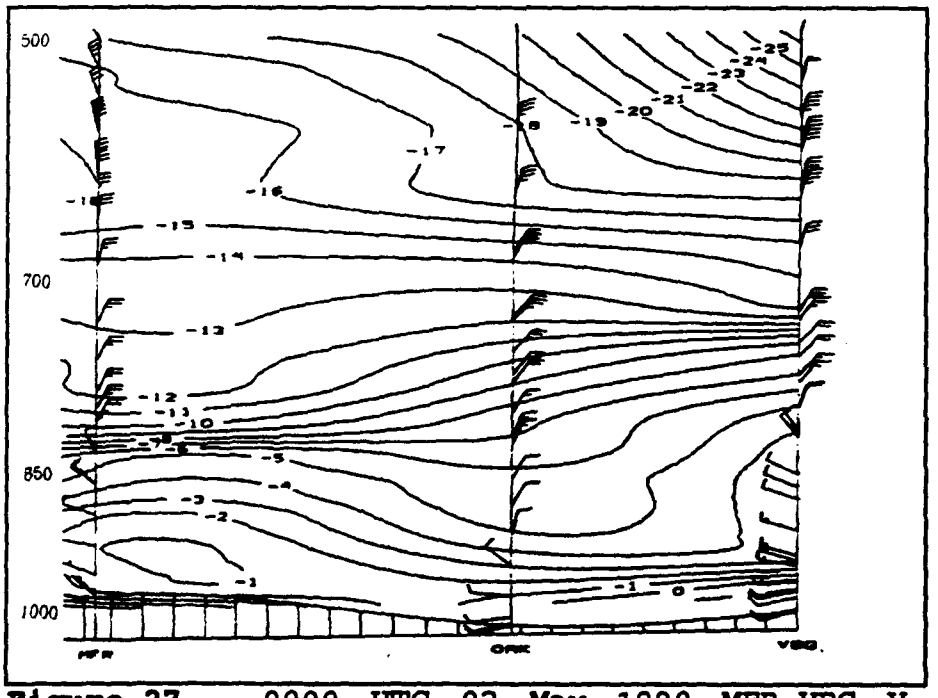

Figure 27. 0000 UTC 02 May 1990 MFR-VBG V-velocity GEMPAK Cross-section Analysis. Northward (m/s, positive). Southward (m/s, negative).

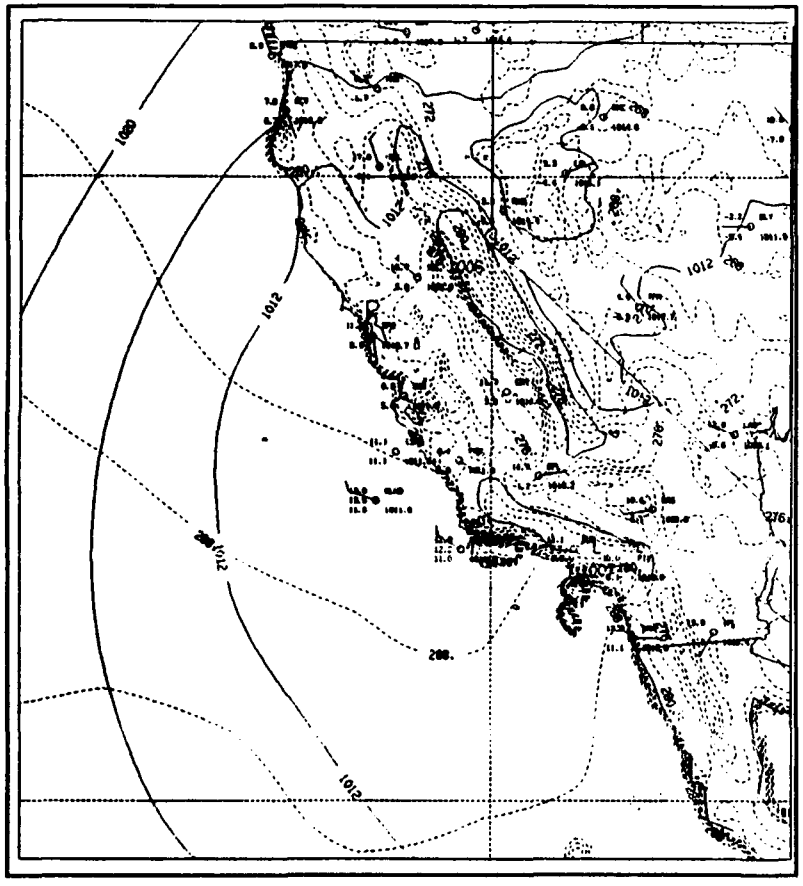

Figure 28. 12-Hour Sea Level Pressure (mb) Forecast Valid 1200 UTC 02 May 1990.

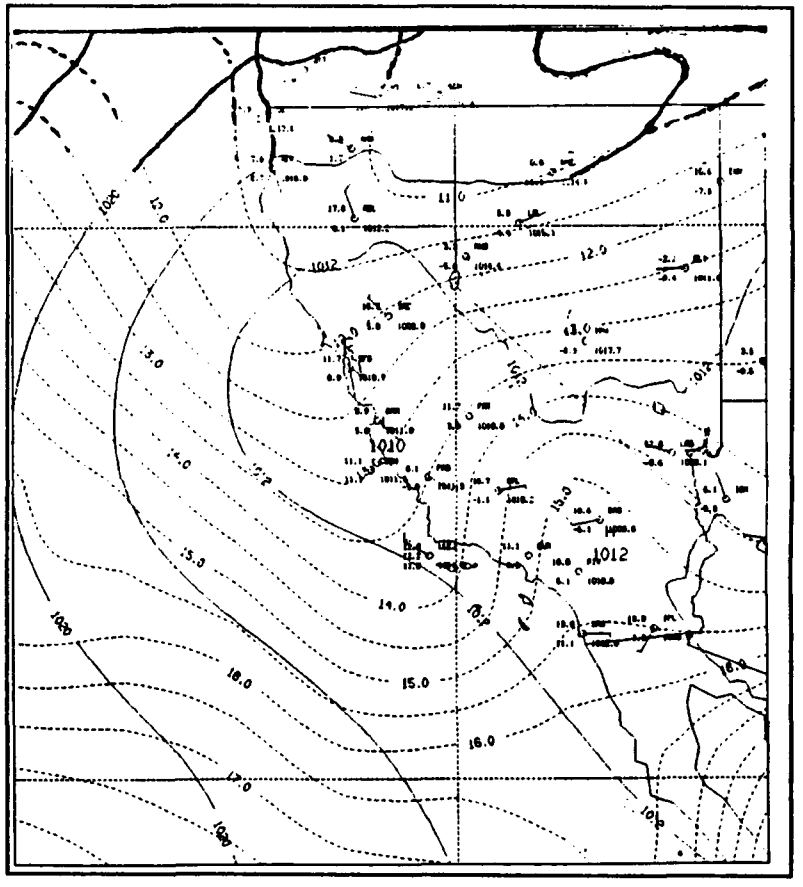

Figure 29. 1200 UTC 02 May 1990 Sea Level Pressure (mb) Analysis.

southern California coast whereas the analysis shows weak ridging through the same area. A lack of data in the region precludes verifying either the model or analysis.

Over land, as expected, the model shows considerable more structure. Low pressure regions over the Santa Ynez and Sierra Nevada Mountains, however, appear to be artifacts of the model's sea level pressure conversion algorithm and are not supported by station data. Within the San Joaquin Valley, pressure gradient is too flat to discern verifiable features. Elsewhere, model output appears reasonable.

Temperature fields over water are nearly identical for both the model and interpolated analysis. Over land, model surface temperatures also look reasonable. As expected for 1200 UTC early morning hours, ground temperature is significantly cooler than SST. The highest surface temperatures are found at low elevations (in the valleys), lowest temperatures at the highest elevations.

b. 850 Mb Constant Pressure

Model height fields (Figure 30) show the same broad scale troughing over the south central portion of the domain as the surface pressure output. Observed heights (Figure 31) at VBG, NTD, LIO and NSI suggest the interpolated analysis more closely represents actual height fields, as expected from a 00-hour analysis versus a 12-hour forecast. The model's

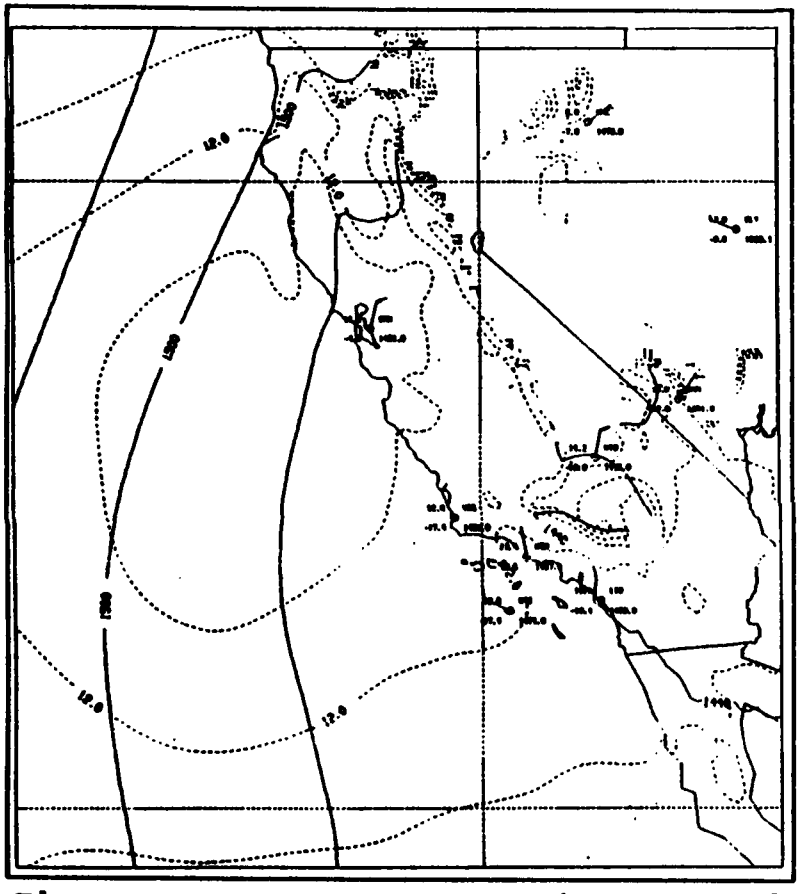

Figure 30. 12-Hour 850 mb Height (m) and Temperature (°C) Forecast Valid 1200 UTC 02 May 1990.

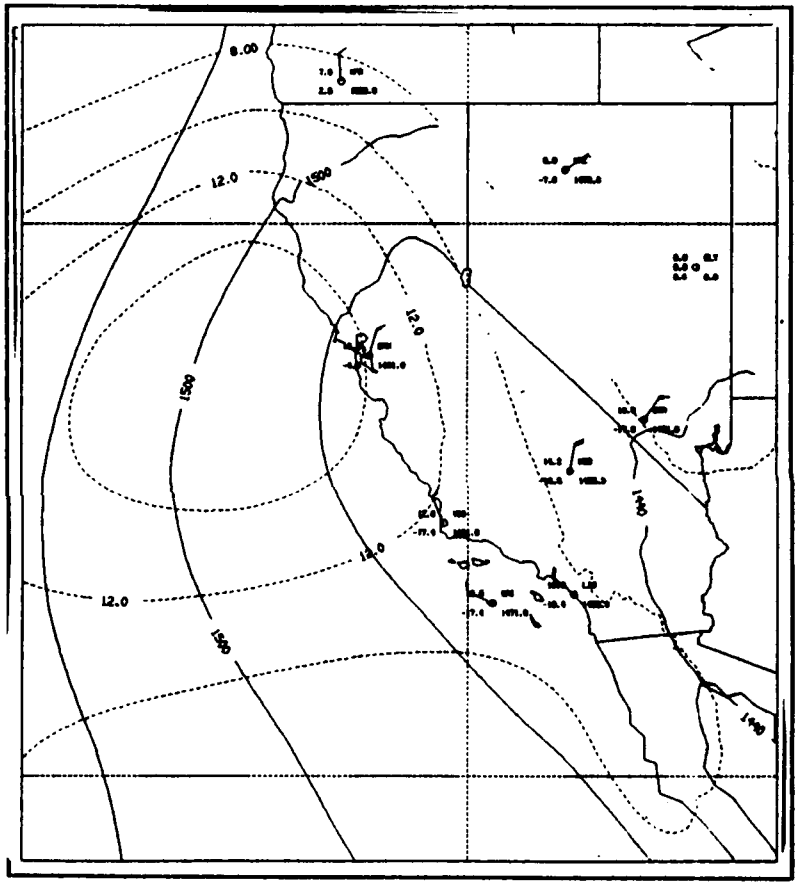

Figure 31. 1200 UTC 02 May 1990 850 mb Height (m) and Temperature (°C) Analysis.

temperature field, however, appears to more closely represent observed conditions than the interpolated analysis.

Wind fields (Figures 32 and 33) are better represented by model output over rough terrain (NID, DRA, WMC) whereas the analysis is better along the coast (OAK, VBG, NTD, LIO, and NSI).

c. 700 Mb Constant Pressure

In general, model and analysis height fields (Figures 34 and 35) agree both with each other and with observations. The only significant difference lies in the southern part of the domain over water where the analysis shows more ridging than the model. Again, little data is available to support either representation. With regard to the temperature fields, neither the analysis nor model can be preferred based solely on station data. However, as at 850 mb, the model shows much more temperature structure than the analysis.

Winds fields (Figures 36 and 37) show two major differences. The analysis shows north-northwest flow in the California bight, the model northerly flow. This disparity reflects the difference in height fields between the two grids. The second difference lies inland over the Sierra Nevada where the model shows topographically induced convergence. Again, the lack of data precludes a determination of whether the model or analysis best represent actual conditions.

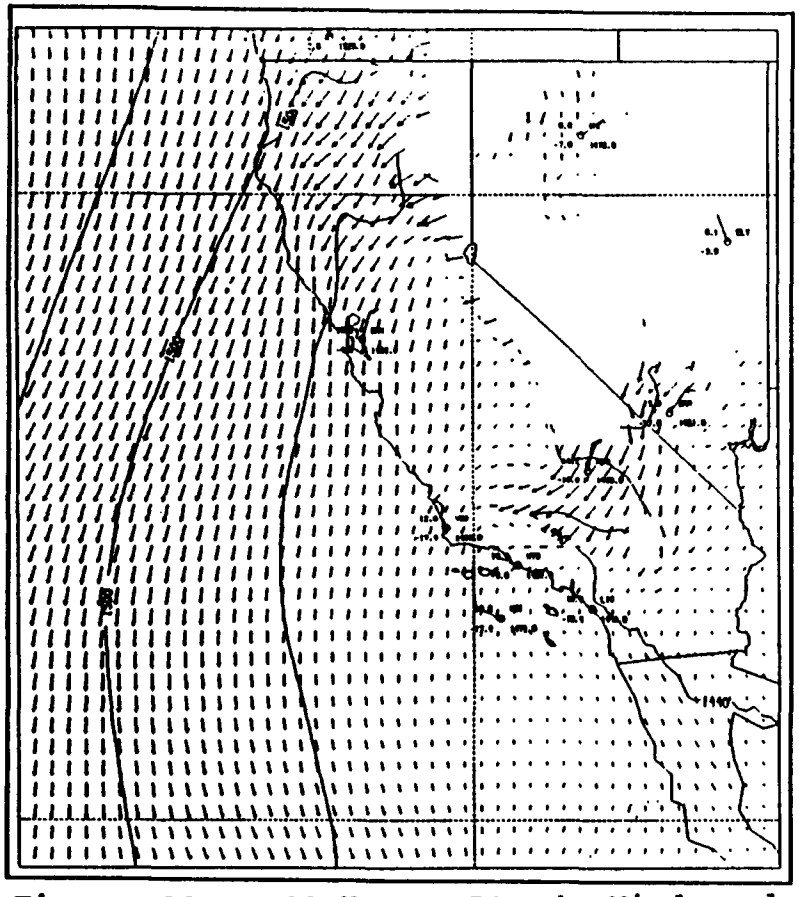

Figure 32. 12-Hour 850 mb Wind and Height (m) Forecast Valid 1200 UTC 02 May 1990.

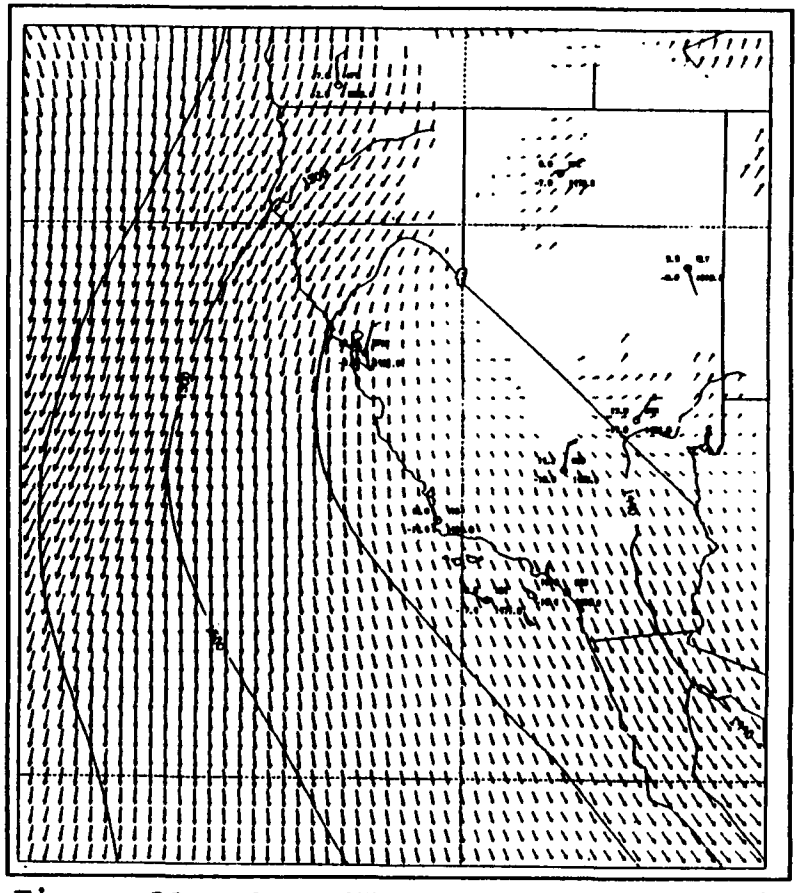

Figure 33. 1200 UTC 02 May 1990 850 mb Wind and Height (m) Analysis.

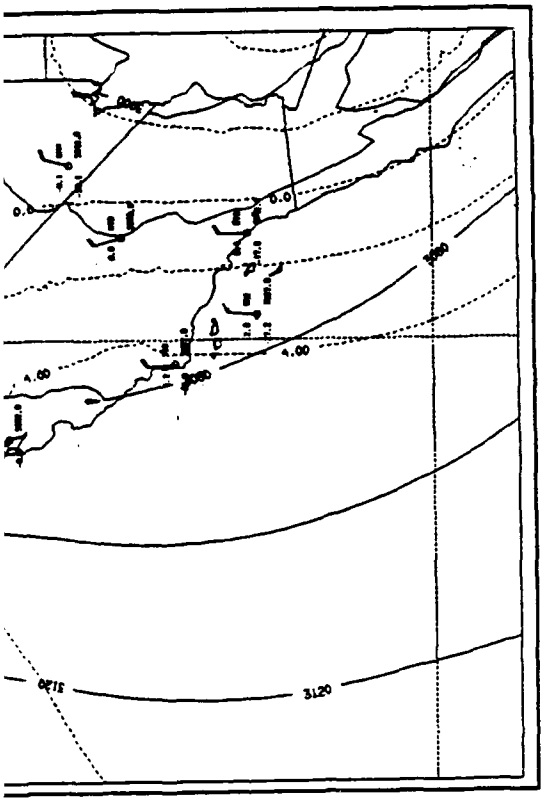

Figure 35. 1200 UTC 02 May 1990 700 mb Height (m) and Temperature (°C) Analysis.

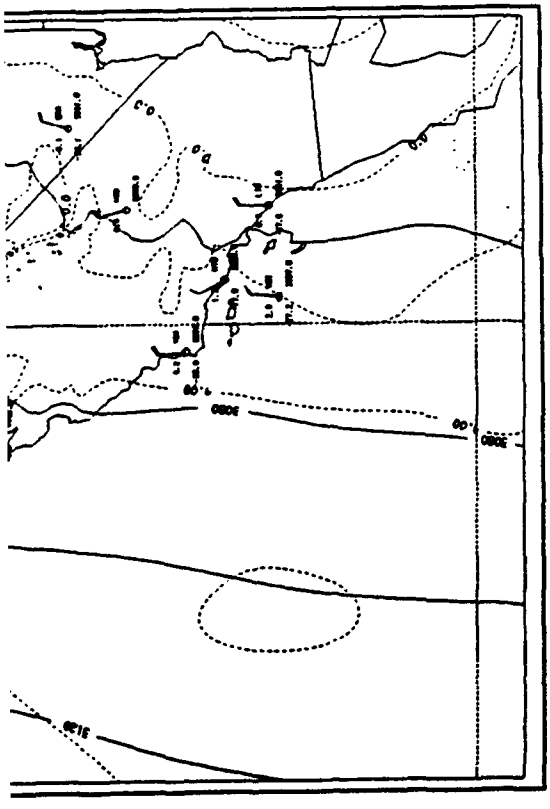

Figure 34. 12-Hour 700 mb Height (m) and Temperature (°C) Forecast Valid 1200 UTC 02 May 1990.

d. 500 Mb (

The pro
alignment in the s
but to a lesser ex
agreement in tempe
(Figures 40 and 4
forecast fields to
NSI, and NID sugges
better represents a

2. Cross-sect

a. MFR to

Figures
temperature cross-s
feature in the GEN
layer below a therm
to NSI. This featu

There is also
depicted by both t
regard to the u-cc
both cross-sectior
Above the inversi
easterly wind maxi
towards VBG and NS
aloft between 700
this feature.

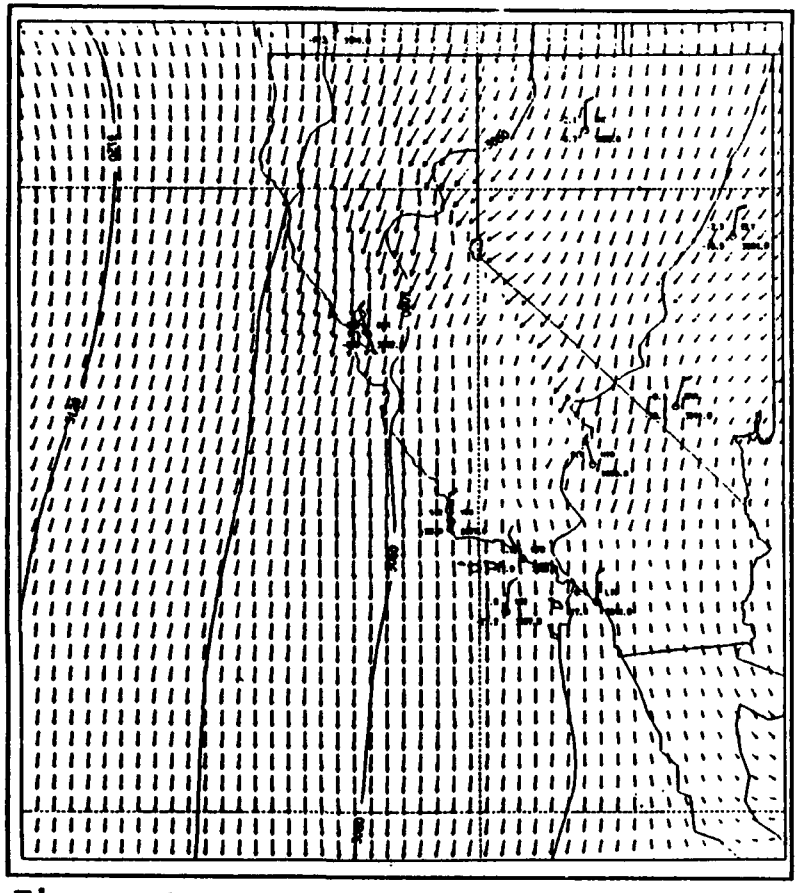

Figure 36. 12-Hour 700 mb Wind and Height (m) Forecast Valid 1200 UTC 02 May 1990.

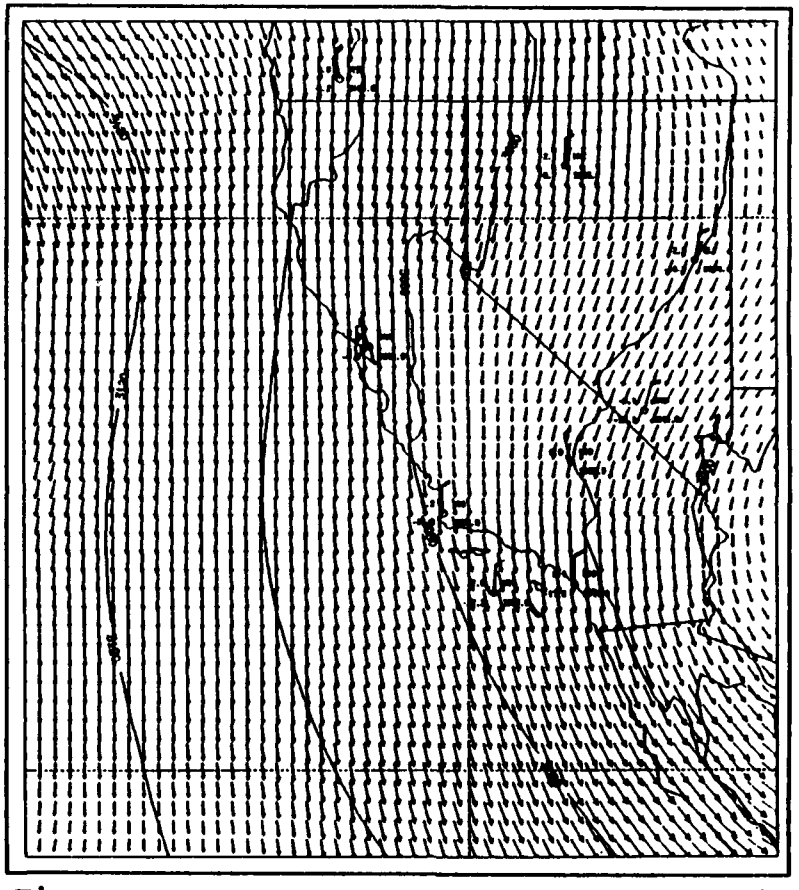

Figure 37. 1200 UTC 02 May 1990 700 mb Wind and Height (m) Analysis.

d. 500 Mb Constant Pressure

The problem of height field (Figures 38 and 39) alignment in the southern part of the domain still persists, but to a lesser extent. Both model and analysis show good agreement in temperature (Figures 38 and 39) and wind fields (Figures 40 and 41). As expected when comparing 12-hour forecast fields to analysis fields, the observed winds at VBG, NSI, and NID suggest that the analysis, rather than the model, better represents actual conditions.

2. Cross-section Analyses

a. MFR to NSI

Figures 42 and 43 show GEMPAK and model potential temperature cross-sections, respectively. The most important feature in the GEMPAK analysis is a strong stable boundary layer below a thermal inversion near 900 mb from north of OAK to NSI. This feature is successfully replicated by the model.

There is also a general similarity in the wind patterns depicted by both the GEMPAK and model cross-sections. With regard to the u-component of the wind (Figures 44 and 45), both cross-sections show westerlies below the inversion. Above the inversion, the model successfully forecasts the easterly wind maximum over OAK near 900 mb. Further south, towards VBG and NSI, the analysis shows a westerly component aloft between 700 and 800 mb whereas the model only hints at this feature.

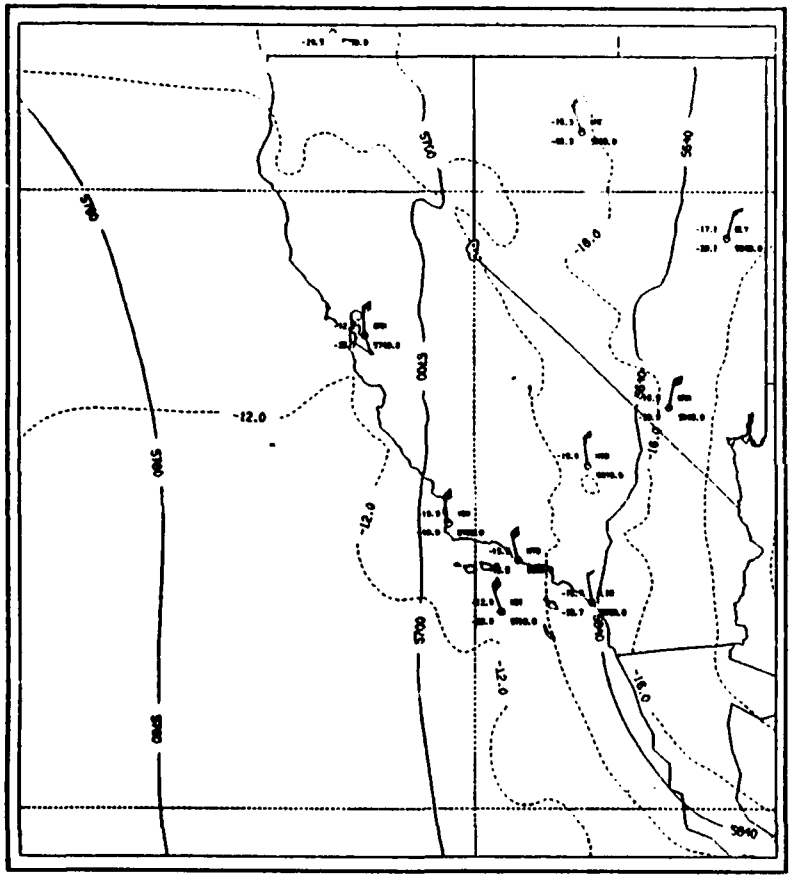

Figure 38. 12-Hour 500 mb Height (m) and Temperature (°C) Forecast Valid 1200 UTC 02 May 1990.

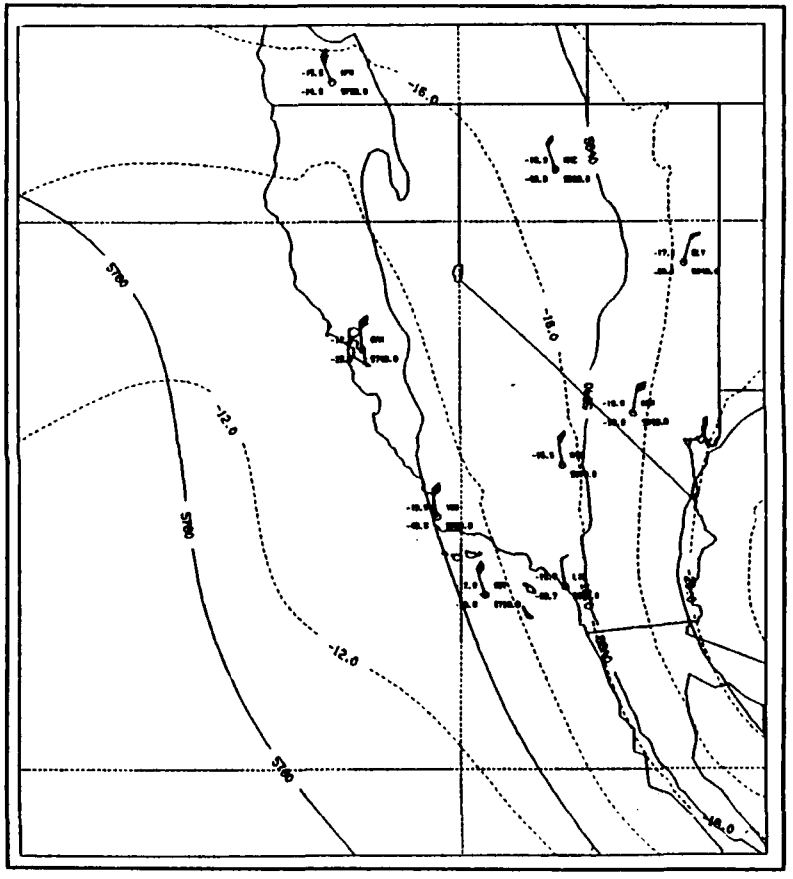

Figure 39. 1200 UTC 02 May 1990 500 mb Height (m) and Temperature (°C) Analysis.

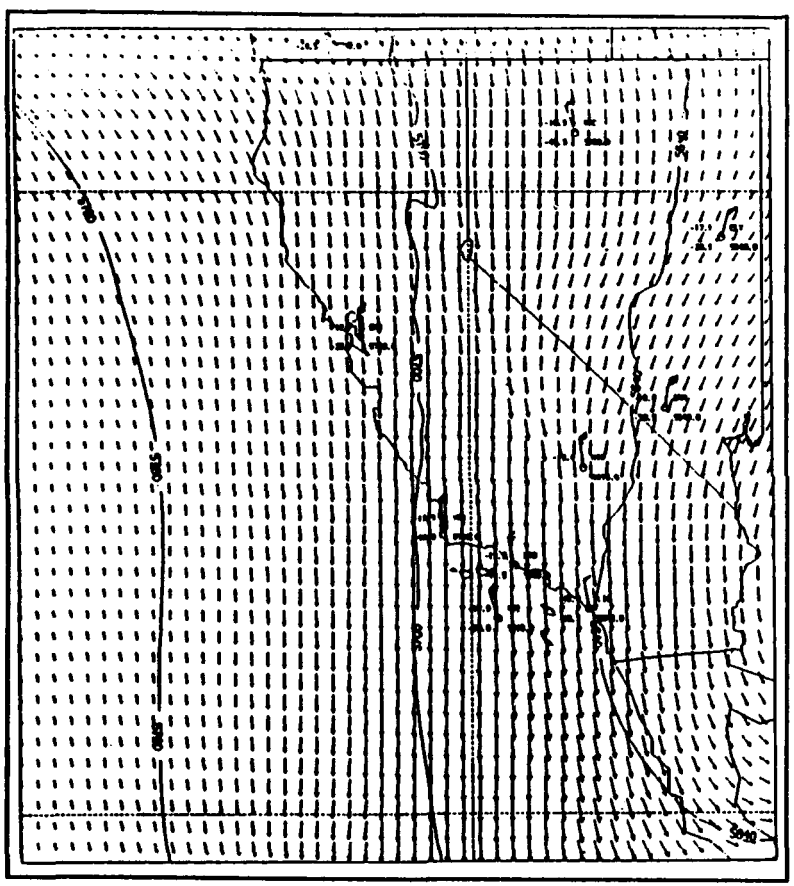

Figure 40. 12-Hour 500 mb Wind and Height (m) Forecast Valid 1200 UTC 02 May 1990.

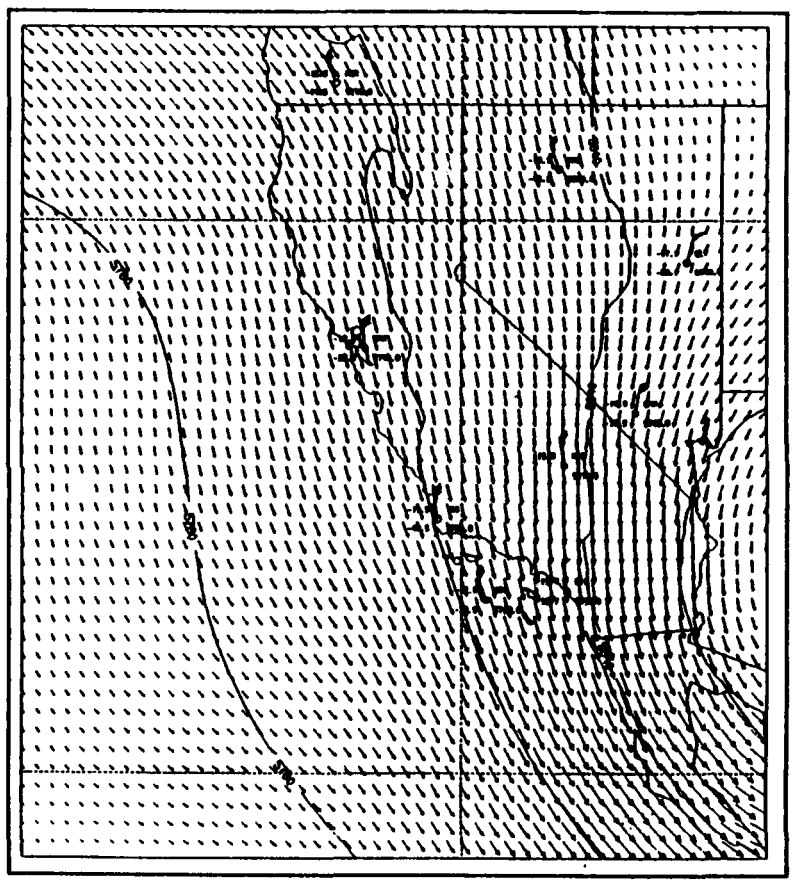

Figure 41. 1200 UTC 02 May 1990 500 mb Wind and Height (m) Analysis.

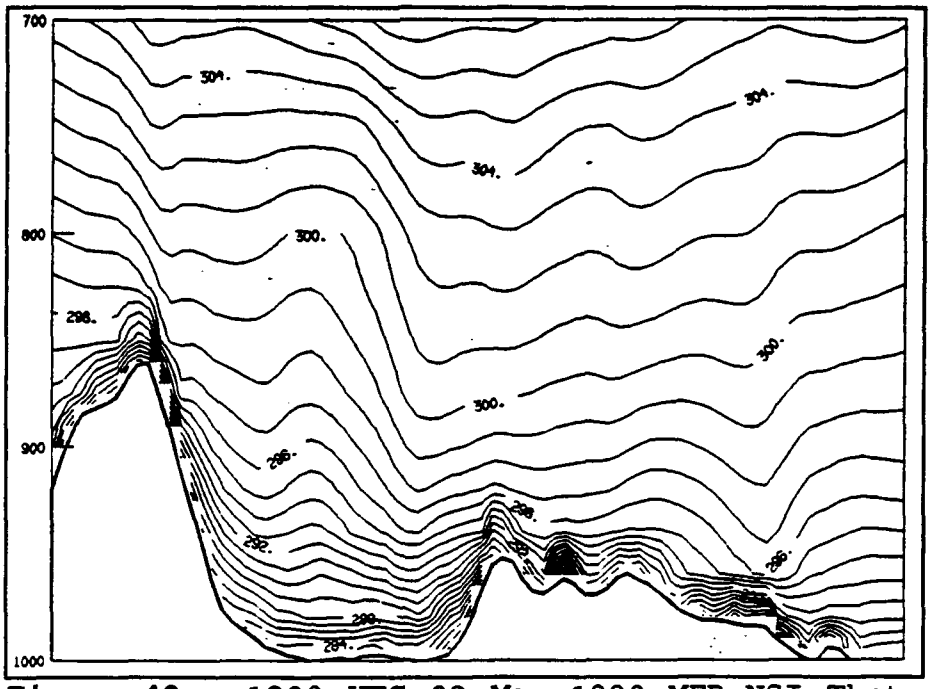

Figure 42. 1200 UTC 02 May 1990 MFR-NSI Theta (°K) Model Output Cross-section Analysis.

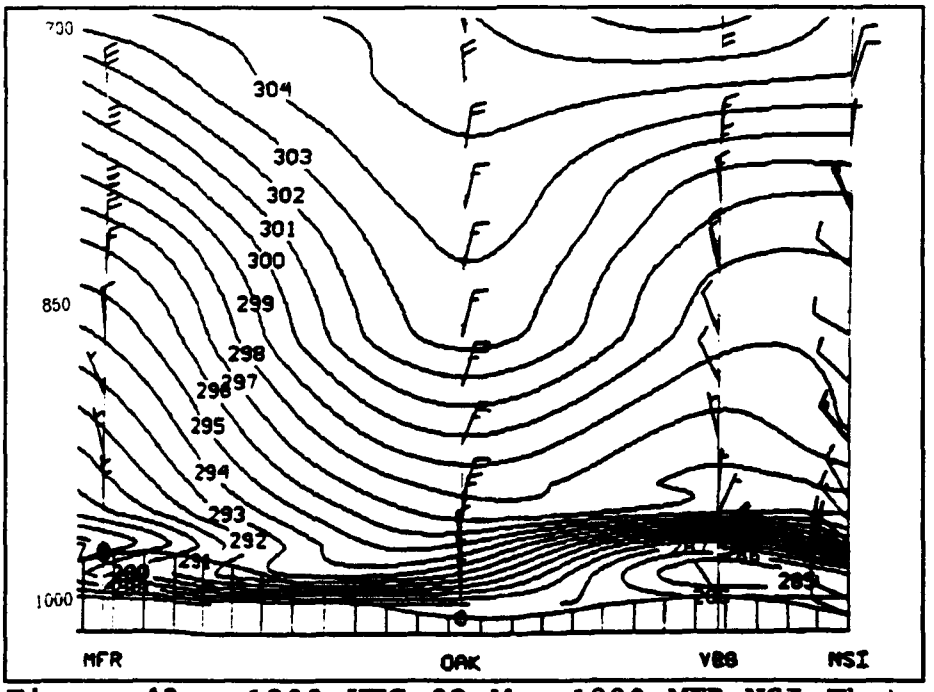

Figure 43. 1200 UTC 02 May 1990 MFR-NSI Theta (°K) GEMPAK Cross-section Analysis.

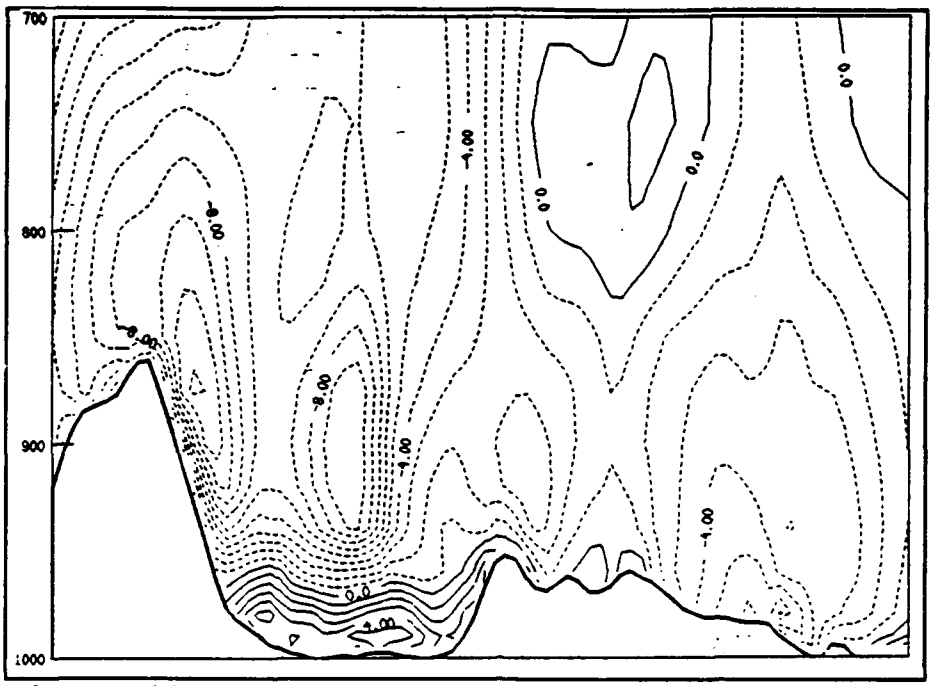

Figure 44. 1200 UTC 02 May 1990 MFR-NSI U-velocity Model Output Cross-section Analysis. Eastward (m/s, solid). Westward (m/s,dashed).

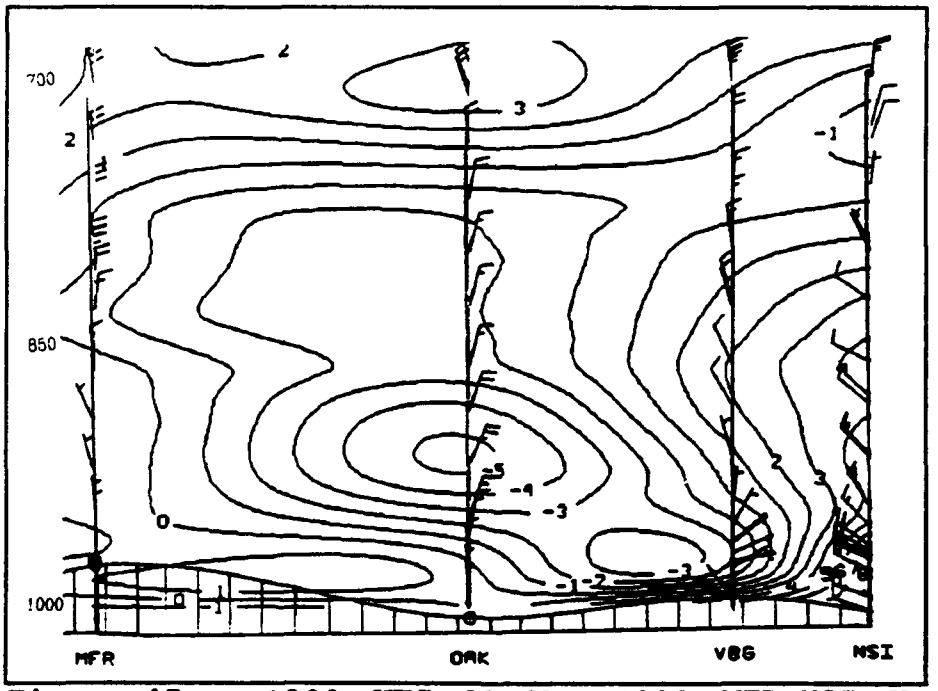

Figure 45. 1200 UTC 02 May 1990 MFR-NSI U-velocity GEMPAK Cross-section Analysis. Eastward (m/s, positive). Westward (m/s,negative).

The v-component cross-sections (Figures 46 and 47) also are generally similar. Northerly flow is prevalent at all levels. Magnitudes are reasonably close; however, the model predicts two wind maxima over OAK, one below 950 mb in the stable layer, the other aloft near 700 mb. The GEMPAK analysis shows only one wind maximum near 875 mb.

Both model (Figures 48) and GEMPAK moisture analysis (Figure 49) agree fairly well both in pattern and magnitude.In particular, both depict more moisture at low-levels; aloft, both show the general trend of moisture decreasing north to south.

b. NSI to ELY

Dramatic changes in topography along this cross-section preclude a complete GEMPAK analysis at lower levels. Still, enough of the analysis is complete to allow evaluation of model performance.

Model (Figure 50) and GEMPAK (Figure 51) potential temperature analyses show comparable structure above the PBL. Within the PBL, the GEMPAK analysis hints at a strong stable layer west of the mountains between NSI and EDW and over the high plains between DRA and ELY. This layer is replicated by the model.

U-component cross-sections (Figures 52 and 53) generally agree above 800 mb and to the east at lower levels, but three differences are worthy of note. First, the model does not

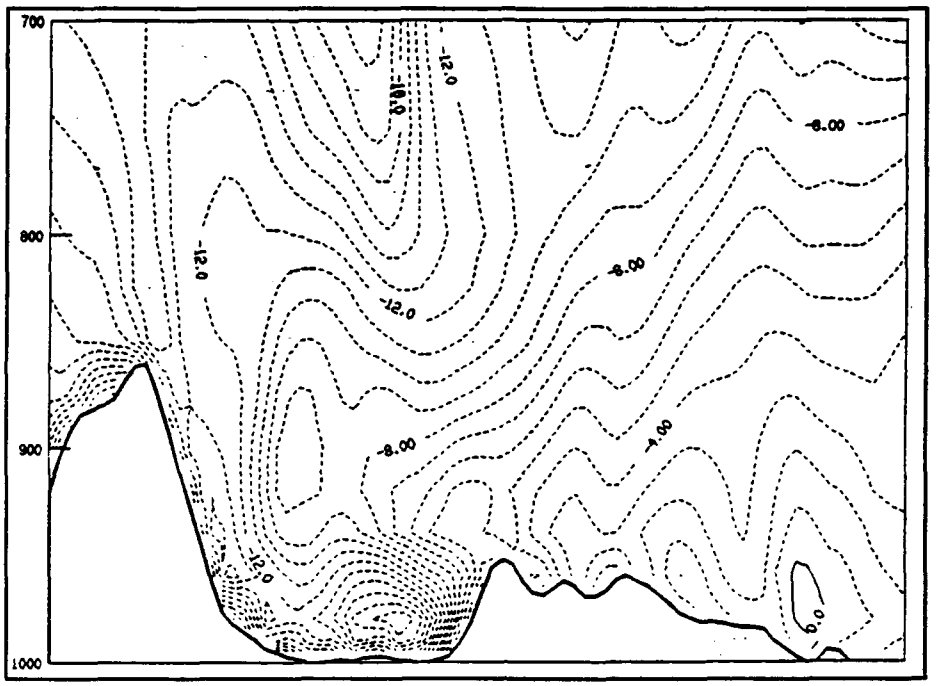

Figure 46. 1200 UTC 02 May 1990 MFR-NSI V-velocity Model Input Cross-section Analysis. Northward (m/s,solid). Southward (m/s, dashed).

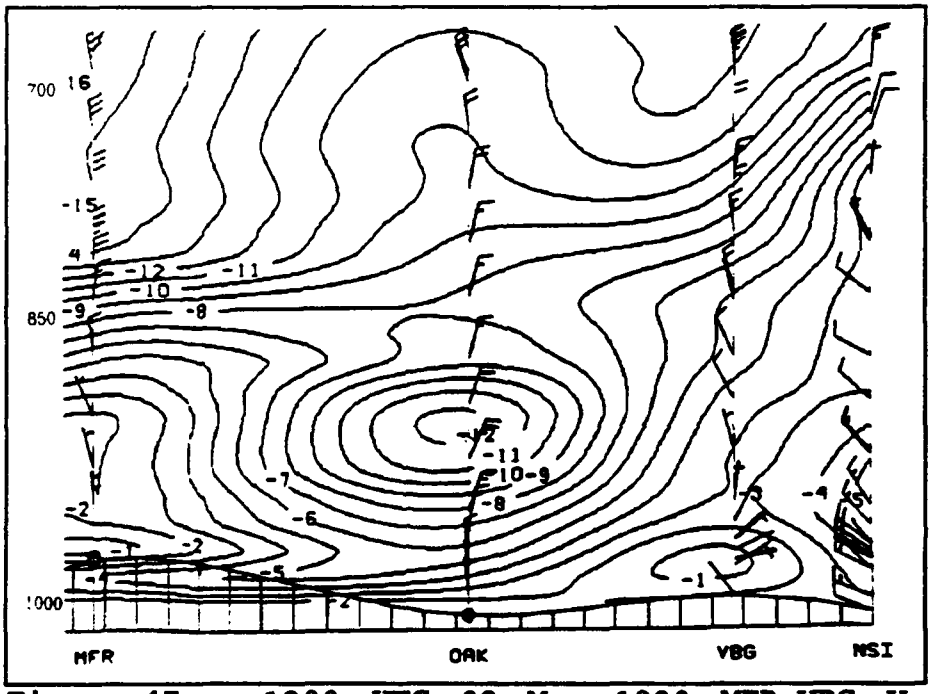

Figure 47. 1200 UTC 02 May 1990 MFR-VBG V-velocity GEMPAK Cross-section Analysis. Northward (m/s, positive). Southward (m/s, negative).

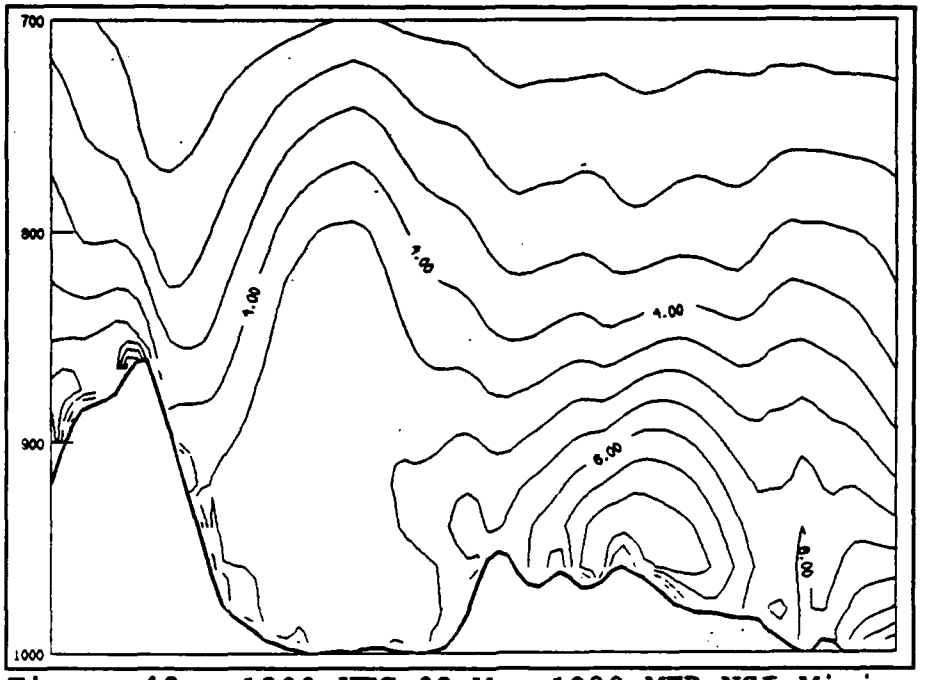

Figure 48. 1200 UTC 02 May 1990 MFR-NSI Mixing Ratio (g/kg) Model Output Cross-section Analysis.

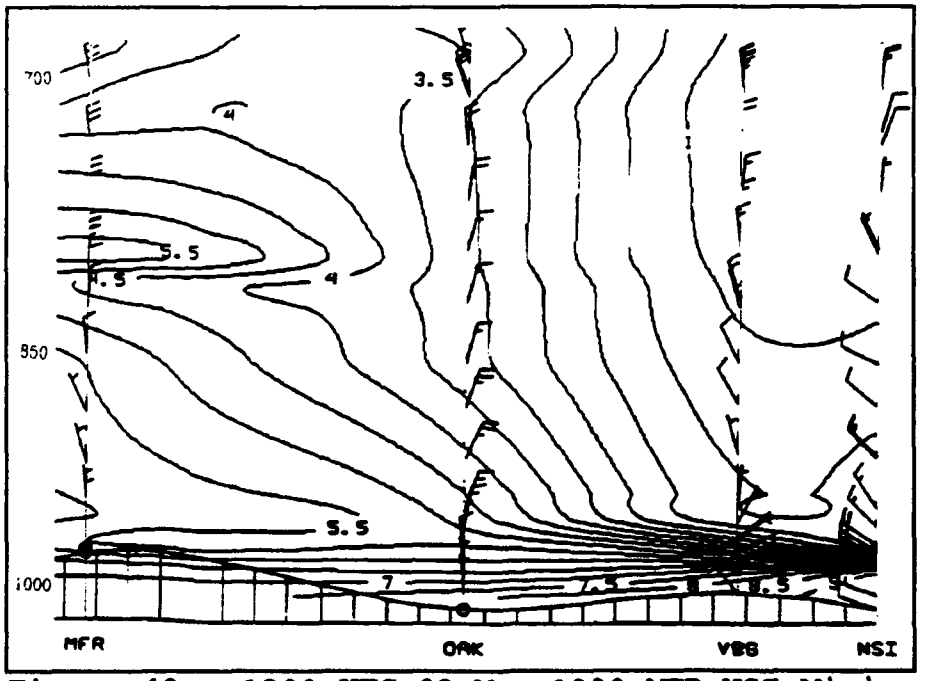

Figure 49. 1200 UTC 02 May 1990 MFR-NSI Mixing Ratio (g/kg) GEMPAK Cross-section Analysis.

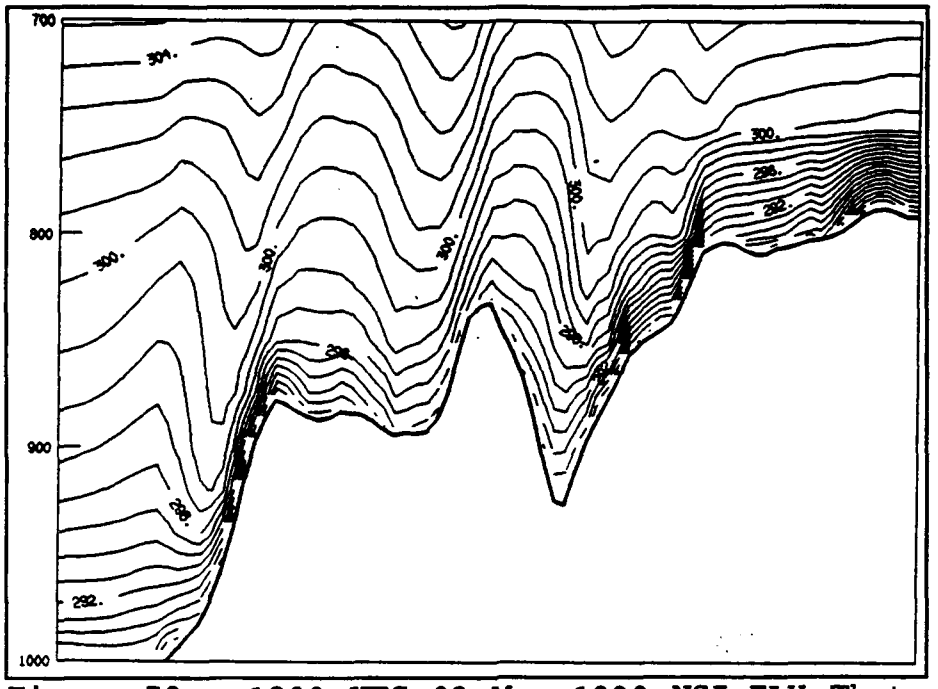

Figure 50. 1200 UTC 02 May 1990 NSI-ELY Theta (°K) Model Output Cross-section Analysis.

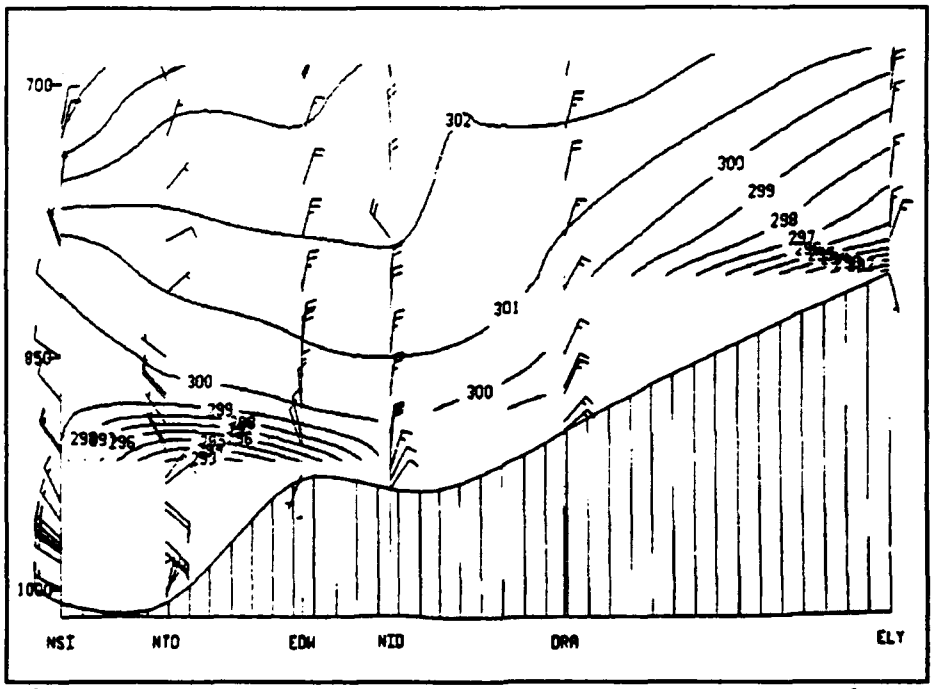

Figure 51. 1200 UTC 02 May 1990 NSI-ELY Theta (°K) GEMPAK Cross-section Analysis.

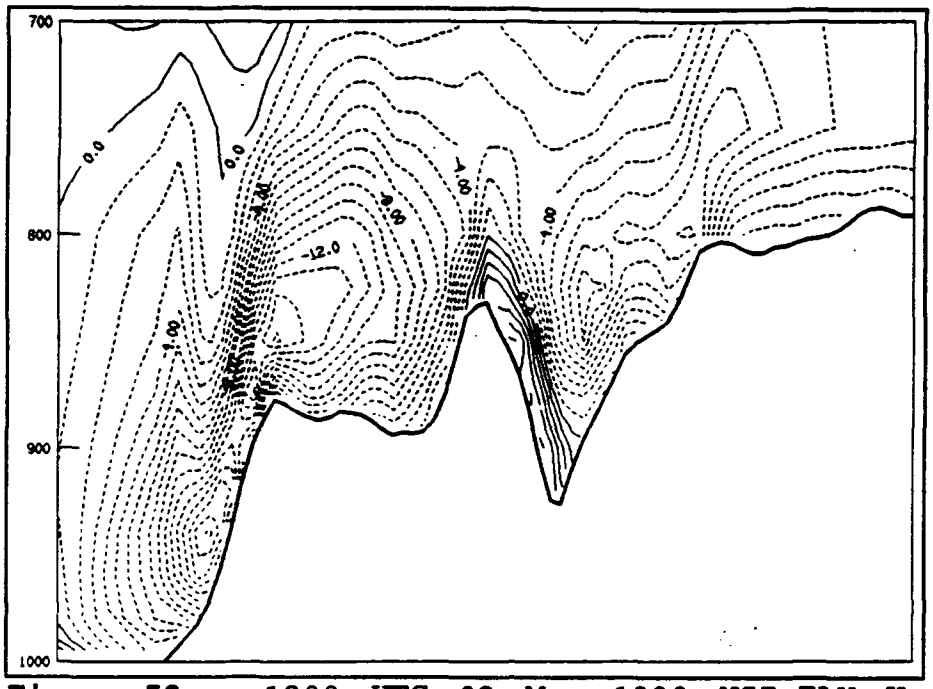

Figure 52. 1200 UTC 02 May 1990 NSI-ELY U-velocity Model Output Cross-section Analysis. Eastward (m/s, solid). Westward (m/s, dashed).

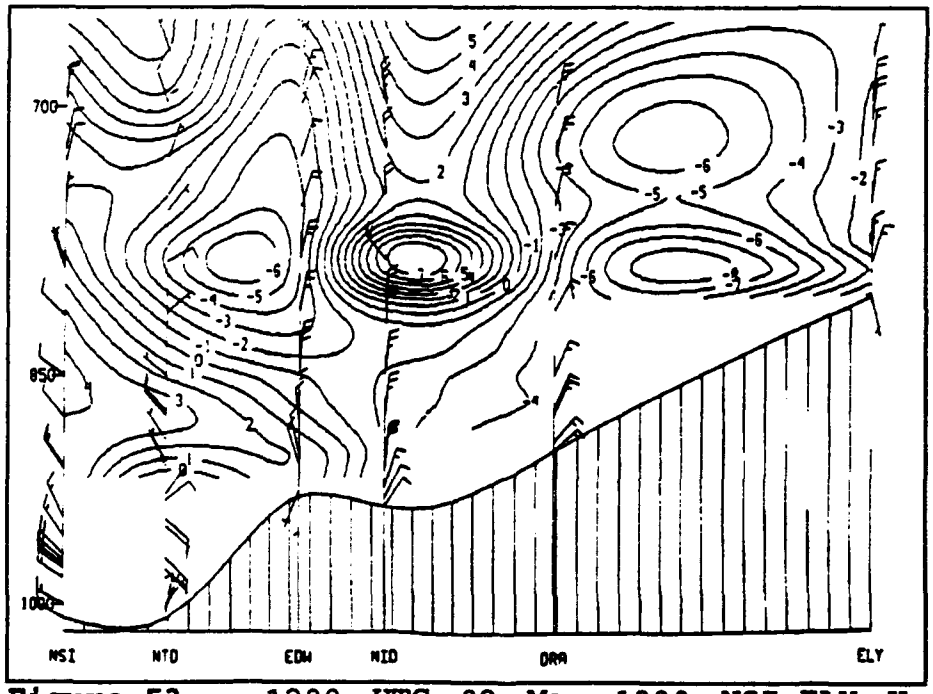

Figure 53. 1200 UTC 02 May 1990 NSI-ELY U-velocity GEMPAK Cross-section Analysis. Eastward (m/s, positive). Westward (m/s, negative).

fully estimate the westerly component at NSI below 800 mb. It shows westerlies only at very low levels (below 950 mb), although it tries to capture the pattern by depicting light easterlies in that region. Second, the GEMPAK analysis shows a westerly maximum over NID at 800 mb. This wind maximum is the result of a misreported wind direction at that level. Last, the model shows a region of strong low level easterlies along the windward slope of the coastal mountain range. No data is available to verify the existence of this feature.

V-component cross-sections (Figures 54 and 55) are in good agreement. The general pattern of lower wind speeds to the east and west is adequately depicted by the model. No major disparities are evident.

The model's moisture cross-section shows considerably higher mixing ratio values than analyzed, possibly a result of poor initial moisture input fields.

3. Vertical Profiles

Vertical profiles from all upper air observations made within the model's domain at 1200 UTC 02 May 1990 were compared with vertical profiles obtained from model output at their locations. Figures 56 through 59 show observed vertical profiles versus profiles of model output for two of these upper air reporting locations, NSI and ELY. These sites not only display typical model output characteristics but are

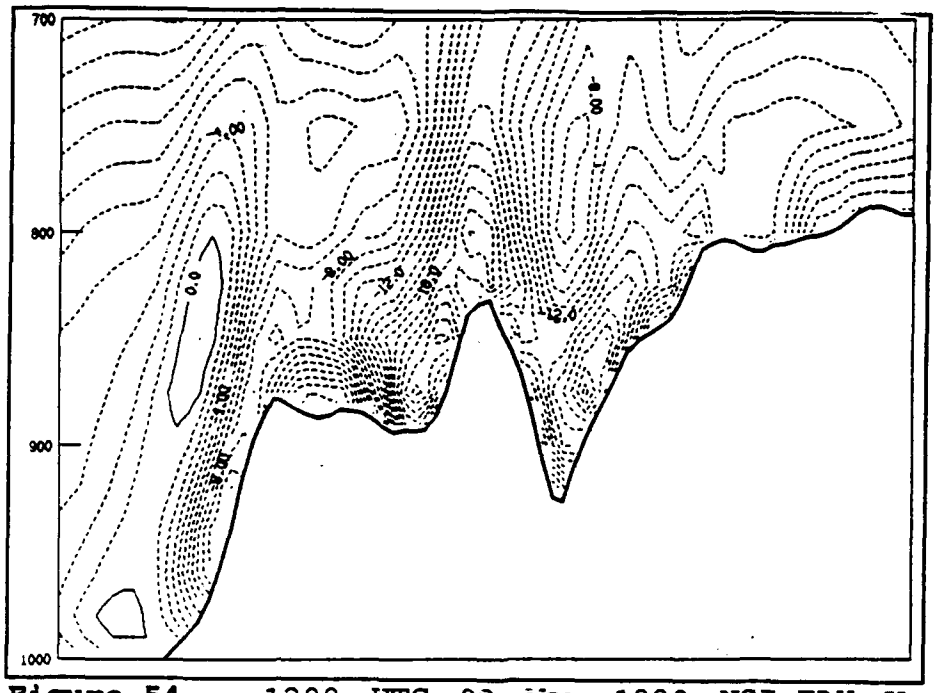

Figure 54. 1200 UTC 02 May 1990 NSI-ELY V-velocity Model Output Cross-section Analysis. Northward (m/s, solid). Southward (m/s, dashed).

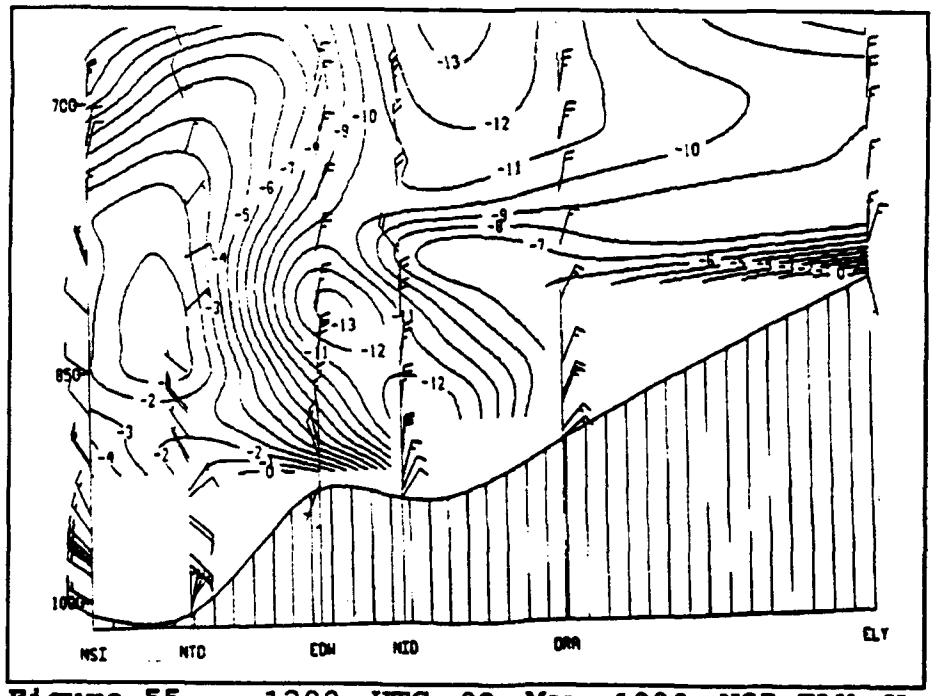

Figure 55. 1200 UTC 02 May 1990 NSI-ELY V-velocity GEMPAK Cross-section Analysis. Northward (m/s, positive). Southward (m/s, negative).

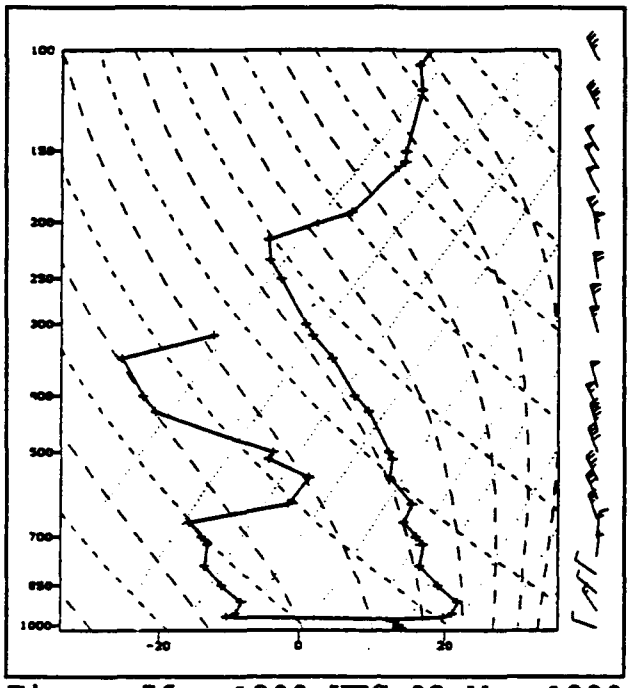

Figure 56. 1200 UTC 02 May 1990 NSI Observed Vertical Profile. (Pressure, mb). (Temperature and Dew Point, °C)

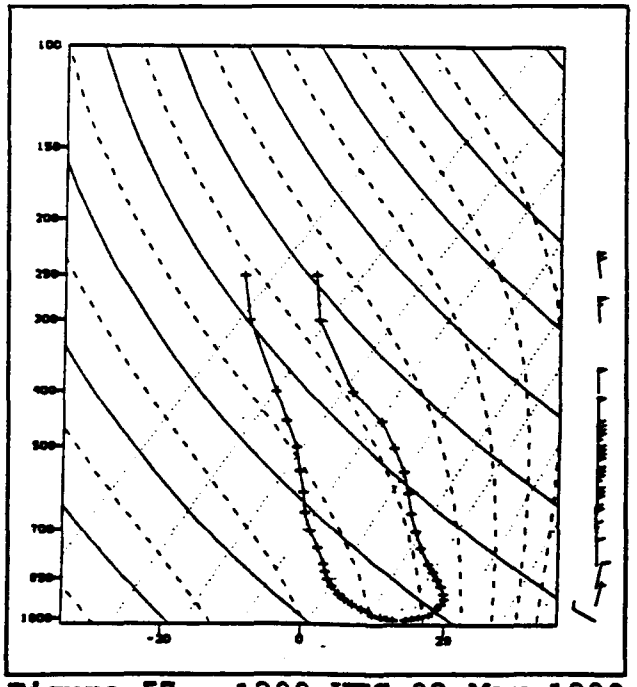

Figure 57. 1200 UTC 02 May 1990 Model Vertical Profile at NSI. (Pressure, mb). (Temperature and Dew Point, °C).

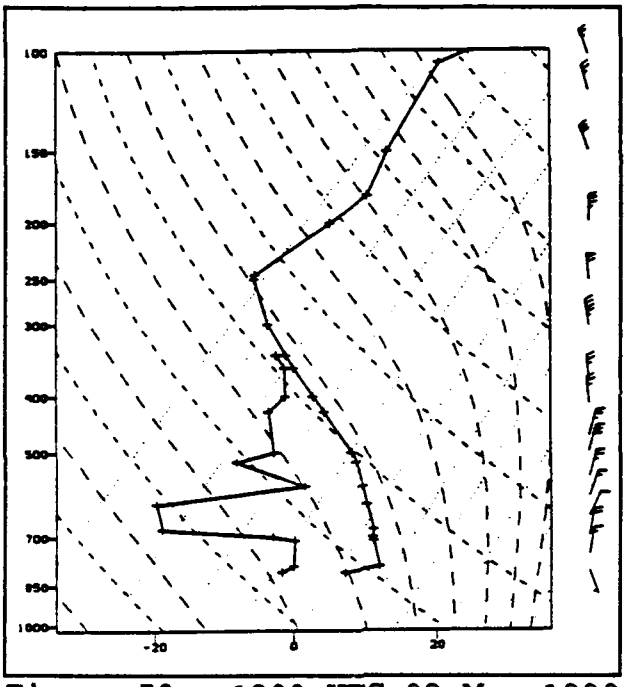

Figure 58. 1200 UTC 02 May 1990 ELY Observed Vertical Profile. (Pressure, mb). (Temperature and Dew Point, °C).

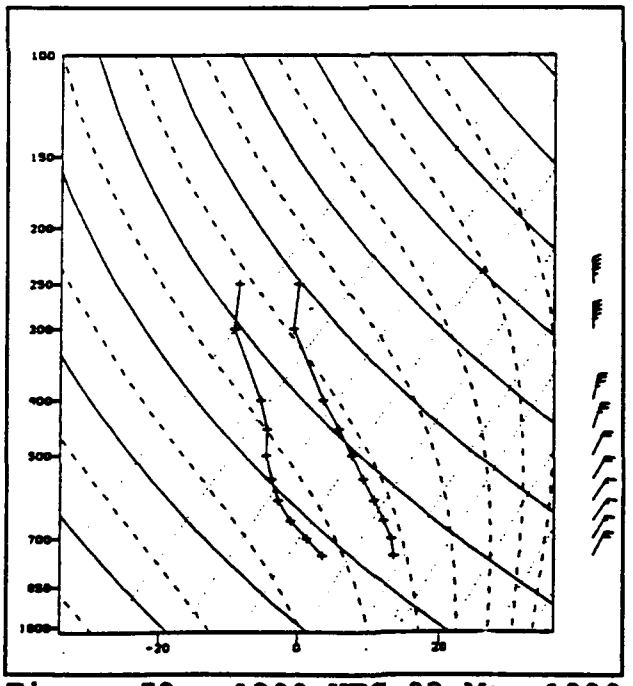

Figure 59. 1200 UTC 02 May 1990 Model Vertical Profile at ELY. (Pressure, mb). (Temperature and Dew Point, °C).

representative of the synoptic and geographic diversity within the model's domain.

The observed temperature profile at NSI shows, as expected, a strong elevated subsidence inversion with a shallow stratus deck below. The model misses this feature and indicates a comparable strength surface-based inversion and no stratus deck. Above the inversion, the model replicates well the vertical thermal structure. Moisture profiles are handled poorly by the model. The model fails to dry out the atmosphere at the top of the inversion or to depict finer scale features aloft. Except for the winds directly above the inversion, model wind profiles are within 5 kts and 20 degrees of observed winds at all levels.

The model is also evaluated at ELY, an inland mountain station. As with the NSI, temperature profiles are adequately handled by the model, although the model misses completely the observed nocturnal surface-based inversion. Moisture profiles are marginal and correlate only on the largest scale. Model and observed wind profiles differ by less than 20 degrees and 5 knots at all levels.

D. MODEL OUTPUT AT 0000 UTC 03 MAY 1990

At 0000 UTC 03 May 1990, low-level model (surface and 850 mb) pressure/height fields show discrepancies with the analyses on their orientation in the California bight region. The model overforecasts the intensity of the low pressure

system which dominates most of coastal southern California. Unlike at 1200 UTC 02 May 1990, significant surface pressure differences between model output and both observations and analyzed fields (minus 4-5 mb) are evident within the bight region. Though not as dramatic, forecasted height values at 850 mb differ by minus 15-20 meters from analyzed values.

Forecast temperature fields remain the model's strong suite. Very little difference was noted between model output and observed temperatures, regardless of location or height. This is particularly noteworthy considering the diurnal heating effects which have occurred during the 12 hour integration period.

The model also performs well with regard to wind fields at all levels. Although only eight vertical soundings were available to verify model output, no significant difference between model and observed winds were found.

The model continues to forecast an overabundance of moisture at all levels in the atmosphere. As at 1200 UTC 02 May, the spatial distribution pattern is similar to the analyses, however, the quantity of moisture predicted far exceeds the analyzed values at nearly all locations.

E. MODEL OUTPUT AT 1200 UTC 03 MAY 1990

At the surface, the model continues to overdeepen the low pressure system in central and southern California. Differences of minus 6-7 mbs are noted along the central California

coast, although the contour pattern and alignment in that region correlates well with the analysis. The problem with contour alignment in the southern latitudes of the domain, however, persists.

At 850 mb, observed winds and forecast wind fields are in fair agreement, with closer agreement over the less mountainous regions. Geopotential height fields, like that of surface pressure, are significantly lower than the analysis (15-20 meters). Above 850 mb, the difference between forecast height fields and analyzed heights diminish with elevation.

Again, temperature fields are well forecasted by the model. Both vertical cross-sections and station profiles show fairly good agreement at all levels, although the model was not able to fully capture inversions as well as it had for the previous 24-hour integration time.

No change in the model's general handling of moisture was seen at 1200 UTC 03 May.

V. MODEL PERFORMANCE FOR MESOSCALE PHENOMENA

A. GENERAL

The purpose of the model assessment is to evaluate the model's potential for use in studies of mesoscale coastal and topographically influenced meteorological features. Following the assessment of the model's capability to replicate synoptic scale systems in the last chapter, an evaluation was made of the model's capability to forecast observed mesoscale flow.

Three types of mesoscale atmospheric phenomena were observed along the California coast during the period 0000 UTC 02 May 1990 - 1200 UTC 03 May 1990. These phenomena include sea and land breezes in the vicinity of Monterey, topographically trapped density currents (the southerly surge), and the Catalina Eddy. As discussed in Chapter 3, all three are coastal phenomena which are heavily influenced by local topography. Analyses of each phenomena were made using available observations; however, these observations were limited and in each case the mesoscale features could not fully be described. Still, the analyses were sufficiently detailed to allow viable comparison with model output and thus provide a means to assess model mesoscale performance.

B. LAND/SEA BREEZES AT FORT ORD, MONTEREY, CALIFORNIA

Figure 60 is a time-height series for the observed (dashed lines) and model output (solid lines) of u-wind components at the NPS doppler wind profiler site at Fort Ord, California, during the period 0000 UTC 02 May 1990 - 1200 UTC 03 May 1990. Although the observed winds are a combination of flows at all scales (i.e., synoptic, mesoscale, local), information about the lower limb of the sea breeze can be discerned below 1400 meters. In particular, observed westerly wind maxima (8-10 m/s) at 0000 UTC 02 May and 0000 UTC 03 May (1600 LST) indicate the sea breeze component of the circulation. The upper limb is masked by larger scale flow and not discernable.

Model output (solid lines) does quite well in replicating the time of the sea breeze component of the circulation. Both observed 0000 UTC 02 May 1990 and 0000 UTC 03 May westerly wind maxima are captured by the model, although the magnitude of the model output is considerably less (2-4 m/s) than the observed values. This difference, however, may be caused by small deviations between observations and model output in the larger scale flow field.

Above 1400 meters, the model shows some disagreement with observed winds. These disparities are largely due by small differences (10-15 degrees) between model wind direction and observed wind direction aloft.

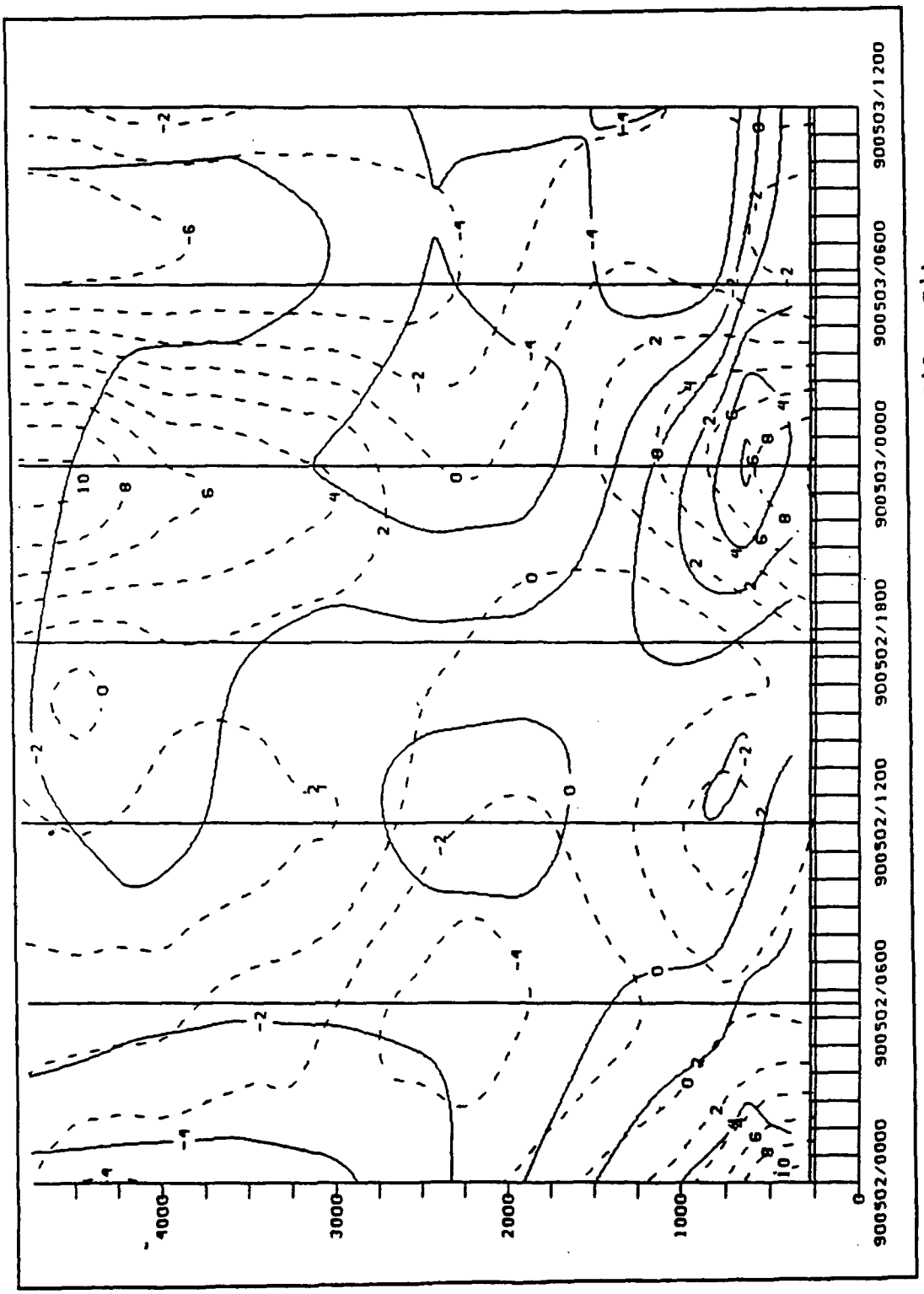

Figure 60. Time/Height Series of U-Component at NPS Profiler Site.

The land breeze at the profiler site sets up with the alignment of the Salinas River Valley from the southeast. The observed v-component time-height series (Figure 61, dashed lines) clearly shows southerly wind maxima near the ground at 1200 UTC (0400 LST) 02 May and 0900 UTC (0100 LST) 03 May. These maxima probably indicate the combined effects of both the land breeze and the southerly surge, with the strongest southerly surge component most likely occurring at 0900 UTC 03 May. It is impossible to clearly identify only the land breeze component of the data so no conclusive verification of the model's land breeze can be made. However, the strong correlation of the timing in diurnal variations between observation and model output (solid lines) clearly shows the model has captured some of the land breeze characteristics.

C. THE SOUTHERLY SURGE ALONG THE CALIFORNIA COAST

Surface southerlies, associated with a weak southerly surge, occurred during the period 0000 UTC 02 May - 1200 UTC 03 May 1990. These southerlies are diurnal in nature, with the strongest observed flow occurring at 1200 UTC (0400 LST) daily. (Modle output indicates strongest southerly coastal flow occurs at 1800 UTC 02 May 1990. No data is available, however, to confirm this output.) This diurnal pattern suggests a link between the strength of the southerly coastal flow, the Catalina Eddy (which also exhibits similar diurnal

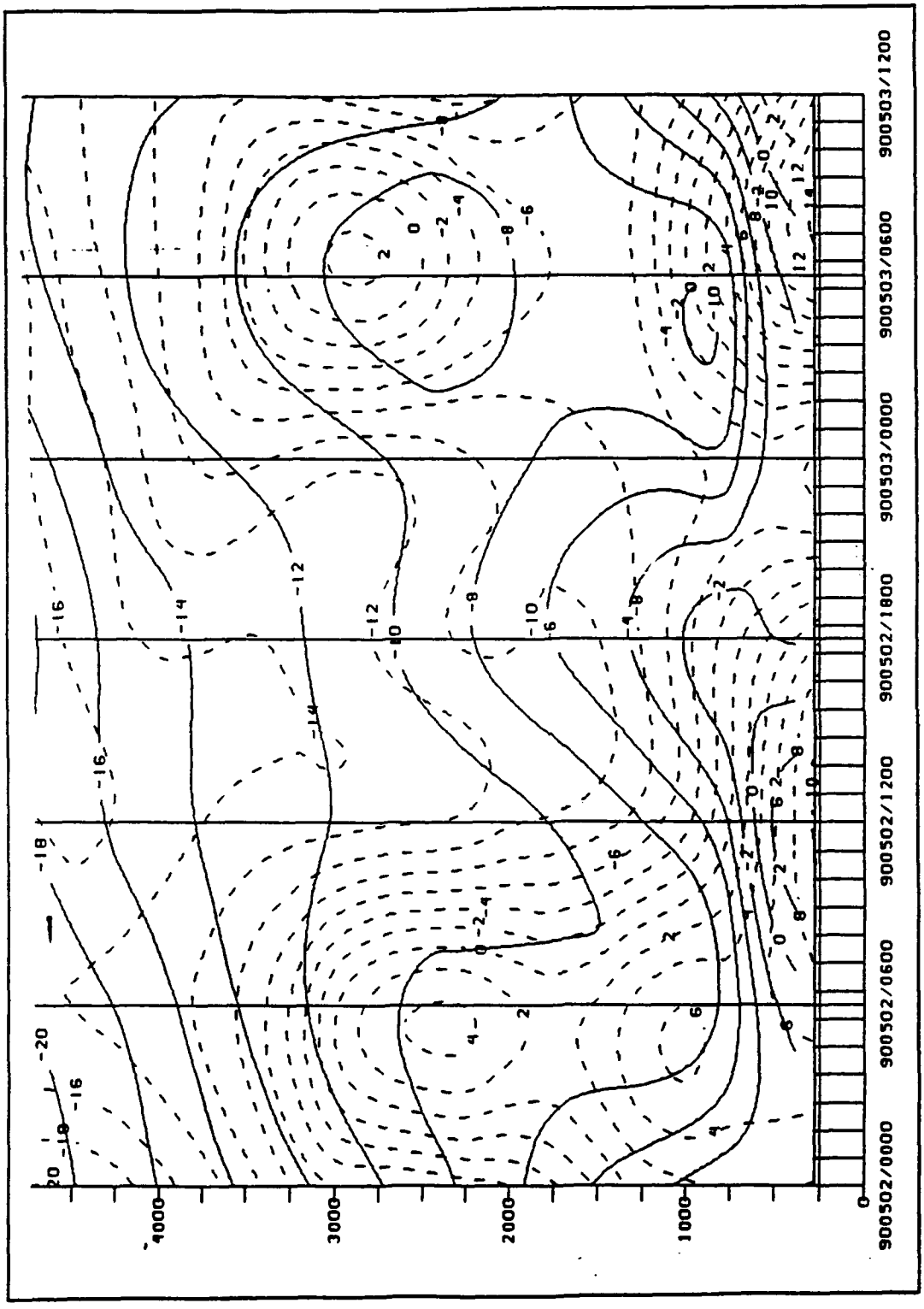

Figure 61. Time/Height Series of V-Component at NPS Profiler Site.

influences), the land/sea breeze along the coast, and possibly the strength of the San Joaquin Valley afternoon thermal low.

Corkill (1991), utilizing a mesoscale analysis scheme based on multi-quadric interpolation, shows the strongest surface southerlies occurred at 1200 UTC 03 May. Figure 3 is his sea level pressure analysis for that time. A narrow band of high pressure extends along the California coast from offshore near Point Conception to Monterey Bay. As indicated in Chapter 3, southerly flow leads to increased marine layer depth. Damming of this cool marine air by the coastal mountain range leads to formation of this mesoscale high pressure feature. Vertical wind profiles at Vandenberg (VBG), from RV PT SUR, and at the NPS profiler site provide additional information on the structure of the surge phenomena at higher levels.

Figure 62 is the model's sea level pressure forecast for 1200 UTC 03 May 1990. The model indicates weak coastal pressure ridging just offshore between Point Conception and Monterey Bay. The model's southerly flow is therefore considerably weaker than the observed flow. There are several explanations for this discrepancy in the model's output.

First, note that the model surface pressures are considerably deeper than observations, an artifact of the model's incorrect forecast of the synoptic height fields discussed in the previous chapter. This incorrect forecast precludes good model replication of the coastal southerlies. As discussed in

Chapter 3, an alongshore pressure gradient with lower pressure to the north is required for ageostrophic coastal southerly flow development. The model's overdeepening of low pressure to the south creates only a weak northward alongshore pressure gradient. Hence, the model's southerly flow is not developed to the same extent as the observed southerly flow.

Second, the modeled coastal terrain is considerably smoother than the actual terrain features. Gaps in the model topography may have "leaked" energy through the coastal range into the interior San Joaquin Valley region. The modeled cold air damming would not be as strong, therefore, as what actually occurred, and the modeled southerly flow would be considerably weaker than observed.

Finally, the inability of the model to adequately develop the marine layer may have contributed significantly to the model's underforecast of the southerly surge's intensity.

Interestingly, the observed VBG sounding shows no southerly wind components at any level during the entire period 0000 UTC, 02 May-1200 UTC, 03 May. This suggests that the ridge lies west of VBG throughout the entire period.

D. TOPOGRAPHICALLY INDUCED GRAVITY WAVES

Observed winds aloft at the NPS profiler site (Figure 61) show relatively strong southerlies at 0600 UTC 02 May and 06 UTC 03 May from the surface to nearly 3500 meters (700 mb). The flow below 1000 meters is most likely associated with the

land breeze. There is a fairly good correlation between the southerly wind maxima near 3000 meters at 0600 UTC and the model's replication of the flow trend (weakened northerly flow) at those same levels and times.

Although no definitive conclusions can be made, the height of these observed southerly wind maxima most likely precludes their association with the low-level southerly flow field. Both OAK 0000 UTC 03 May and RV PT SUR 0600 UTC 03 May 1990 soundings show a weak inversion and significant drying out at that height. These observations, along with the diurnal recurrence of the southerly maxima, indicate that they might be gravity waves on an internal boundary layer at that level. This internal boundary layer could be generated by broad scale northeasterly flow off the Sierra Nevada which manifests itself on the west coast after the thermal low in the San Joaquin Valley is sufficiently weak to allow energy to propagate westward. A similar explanation was offered by Streed (1990) who suggested these anomalies were generated by lower, local topographic features.

E. THE CATALINA EDDY

Mass and Albright (1989) describe the full evolution of a composite Catalina Eddy event. The Catalina Eddy results from the interaction between synoptic scale flow, regional diurnal circulations, and the complex topography surrounding the California bight. Therefore the model's handling of the

Catalina Eddy which occurred during the period 0000 UTC 02 May 1990 - 1200 UTC 03 May 1990 is of particular interest when assessing the model's performance.

Aside from surface observations, only soundings from LIO, NSI, VBG, and NTD were available to define the Eddy structure. These profiles were linearly interpolated to obtain values at model levels. The model's overprediction of low pressure in the bight has already been addressed; therefore, only the model's Eddy wind fields will be evaluated.

At 1200 UTC 02 May 1990, soundings at NSI, LIO and NTD indicate the Eddy vortex was located near Santa Catalina Island. Based on these observations, a closed vortex was suggested at all heights up to 920 mb. The model replicates the depth of the vortex, although it places the vortex center farther south than the analyzed position. Figure 63 shows model output wind fields at 980 mb, midway through the depth of the vortex. There is good agreement between model and observed winds at VBG, NTD, and LIO. The forecast winds at NSI are in error slightly as the model has placed the center of the vortex near San Clemente Island, south of the analyzed center near Santa Catalina.

At 0000 UTC 03 May 1990, the model shows the sea breeze dominating flow in the California bight at all levels up to 875 mbs. Only two reports are available to confirm the model's wind fields, VBG and LIO. Model output winds are in good agreement with these observations. Additionally, the

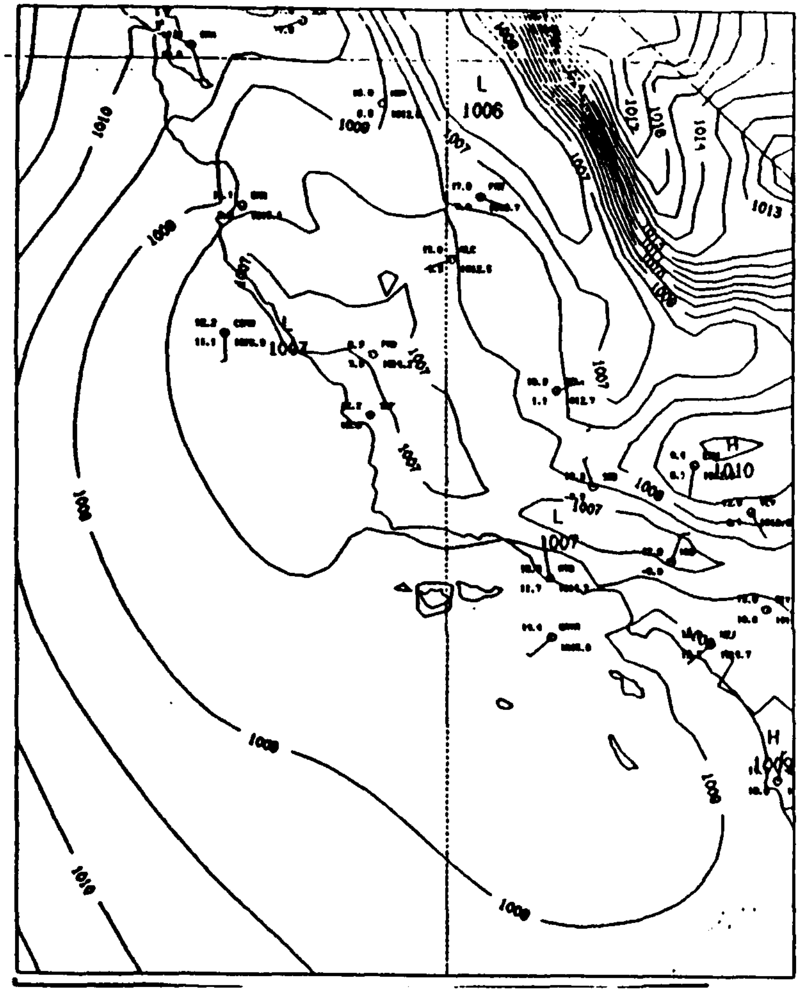

Figure 62. 36-Hour Sea Level Pressure (mb) Forecast Valid 1200 UTC 03 May 1990.

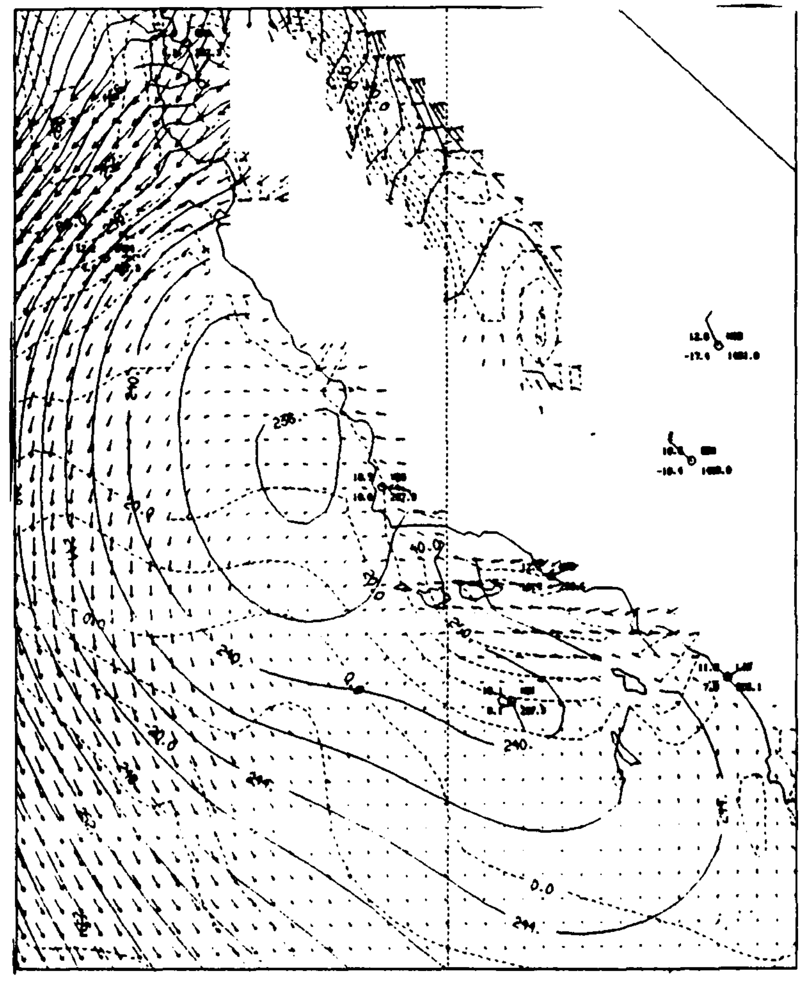

Figure 63. 12-Hour 980 mb Winds, Heights (solid, m) and Relative Vorticity (dashed, 10^{-5}/s) Forecast Valid 1200 UTC 02 May 1990.

model wind fields agree well with the 0000 UTC composite Catalina Eddy of Mass and Albright (1989).

Figure 64 shows 980 mb model wind fields and observations at 1200 UTC 03 May 1990. The few observations available cannot define the location of the Eddy's vortex, however, southerly flow at NSI at 980 mb confirms its existence somewhere southwest of NSI. The model wind fields are very reasonable, and match observed winds at VBG, NTD, LIO, and NSI quite well.

During the period of strongest Catalina Eddy activity (1200 UTC), the model shows a region of stronger offshore flow funneled through the passes between the San Ynez and San Rafeal Mountains at all levels up to 875 mb. The model suggests this flow originates east of the Sierra Nevada, following the terrain as it flows around higher barriers and over the lower topographic features until it reaches the vicinity of the California bight (Figure 65). The existence of this flow pattern is supported by observations at both EDW and NID. Upon reaching the California basin, the wind maximum would have considerable horizontal shear (and associated positive vorticity) over the bight region. The model's 980 mb relative vorticity field at 1200 UTC 03 May (dashed lines, Figure 64) confirms that cyclonic shear vorticity occurs in the California bight. This vorticity could be a possible maintenance or generation mechanism for the Catalina Eddy, and

compliment the lee troughing mechanism postulated by Mass and Albright (1989).

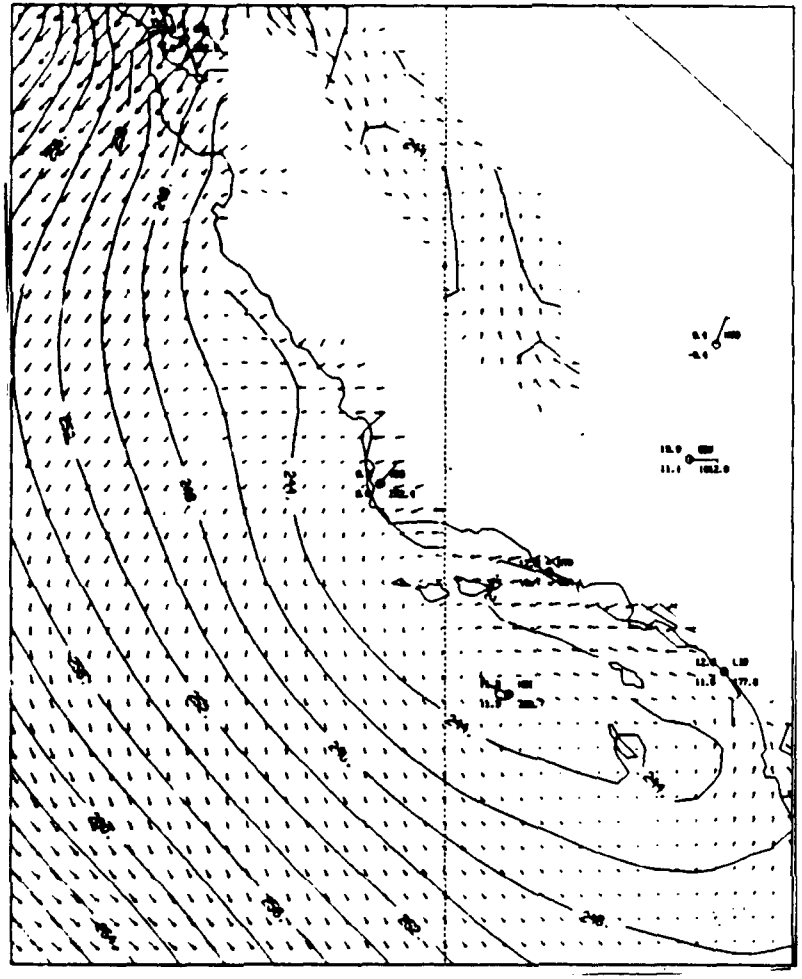

Figure 64. 36-Hour 980 mb Wind and Height (m) Forecast Valid 1200 UTC 03 May 1990.

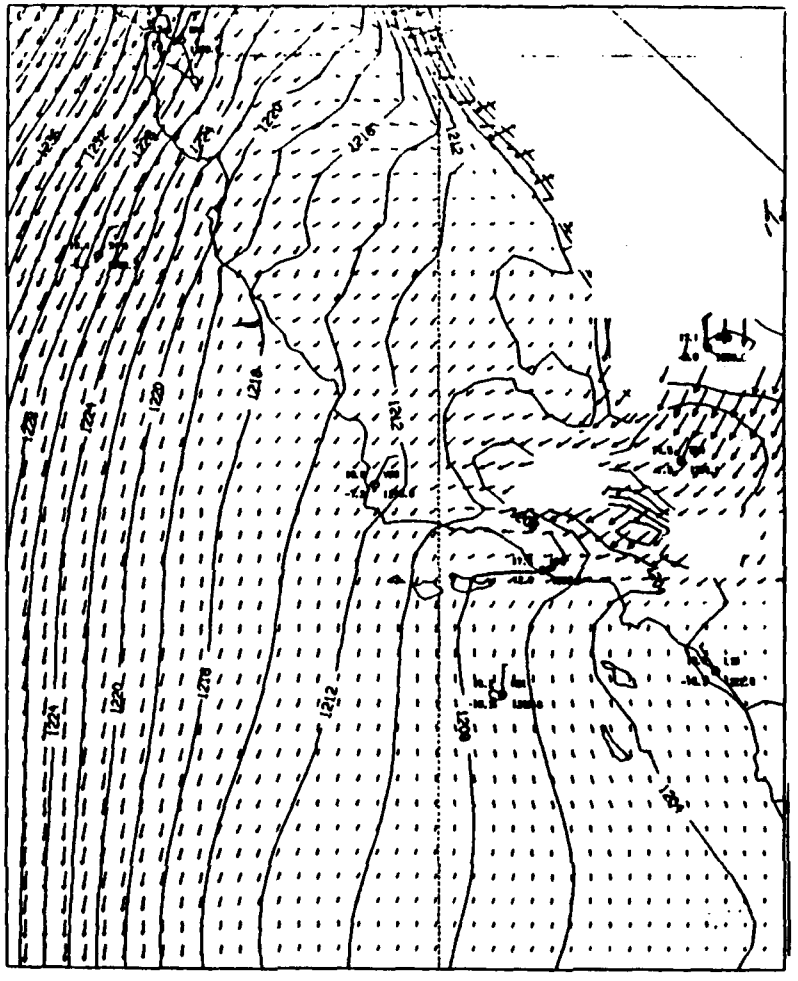

Figure 65. 36-Hour 875 mb Wind and Height (m) Forecast Valid 1200 UTC 03 May 1990.

VI. CONCLUSIONS

This study determined that the NRL Limited Area Dynamical Weather Prediction Model can be used to study mesoscale atmospheric phenomena along the west coast of the United States. In particular, the model successfully replicated three instances of mesoscale coastal phenomena observed in that region during the period 0000 UTC 02 May 1990 to 1200 UTC 03 May 1990. They include land/sea breezes as observed by the Naval Postgraduate School Doppler wind profiler, a Catalina Eddy event, and its associated southerly surge. Although the model had problems with exact replication of near surface low-level inversions, in general model wind and temperatures had only small departures from observed fields. Validation of the height and moisture fields were inconclusive, however, and further work is required.

LIST OF REFERENCES

Anthes, R.A., 1977: A cumulus parameterization scheme utilizing a one-dimensional cloud model. *Mon. Wea. Rev.*, **105**, 270-286.

Arakawa, A., and V.R. Lamb, 1977: Computational design of the basic dynamic process of the UCLA general circulation model. *Methods in Computational Physics*, Vol. 17, Academic Press, 173-265.

Blackader, A.K., 1976: Modeling of the nocturnal boundary layer. Preprints, *Third Symposium on Atmospheric Turbulence, Diffusion and Air Quality*, Raleigh, Amer. Meteor. Soc., 46-49.

Bosart, L.F., 1983: Analysis of a California eddy event. *Mon. Wea. Rev.*, **111**, 1619-1633.

Businger, J.A., J.C. Wyngaard, Y. Izumi and E.F. Bradley, 1971: Flux-profile relationship in the atmospheric surface layer. *J. Atmos. Sci.*, **28**, 181-189.

Chang, S.W., 1979: An efficient parameterization of convective and non-convective planetary boundary layers for use in numerical models. *J. Appl. Meteor.*, **18**, 1205-1215.

Chang, S.W., K. Brehme, R. Madala and K. Sashegyi, 1989: A numerical study of the East Coast snowstorm of 10-12 February 1983. *Mon. Wea. Rev.*, **117**, 1768-1776.

Corkill, P.W., 1991: Synoptic and mesoscale factors influencing stratus and fog in the central California coastal region. M.S. thesis, Meteorology Department, Naval Postgraduate School, Monterey, CA 93943.

Dorman, C.E., 1985: Evidence of Kelvin waves in California's marine layer and related eddy generation. *Mon. Wea. Rev.*, **113**, 827-839.

Gerber, H., S. Chang and T. Holt, 1989: Evolution of a marine boundary layer jet. *J. Atmos. Sci.*, **46**, 1312-1326.

Glendening, J.W., 1985: Modeling the influences of horizontal variations in terrain and temperature on the well-mixed boundary layer. Ph.D. dissertation, University of Washington. [Available from University Microfilms, Ann Arbor, MI 48106.]

Haltiner, G.J., and F.L. Martin, 1972: Dynamical and Physical Meteorology, McGraw-Hill, Inc., 52.

Holt, T., and S. Raman, 1988: A review and comparative evaluation of multi-level boundary layer parameterizations for first order and turbulent kinetic energy closure schemes. *Rev. Geophys.*, **26,** 761-780.

Holt, T., S. Chang and S. Raman, 1990: A numerical study of coastal cyclogenesis in GALE IOP-2: Sensitivity to parameterizations. *Mon. Wea. Rev.*, **118,** 234-257.

Keyser,D., and R.A. Anthes, 1977: The applicability of a mixed layer model of the planetary boundary layer to real-data forecasting. *Mon. Wea. Rev.*, **105,** 1351-1370.

Kuo, H.L., 1974: Further studies of the parameterization of the influences of cumulus convection on large-scale flow. *J. Atmos. Sci.*, **31,** 1232-1240.

Madala, R.V., S.W. Chang, U.C. Mohanty, S.C. Madan, R.K. Paliwal, V.B. Sarin, T. Holt And S. Raman, 1987: Description of the Naval Research Laboratory limited area dynamical weather prediction model. NRL Technical Report 5992. [Available from NRL Washington, D.C. 20375.]

Mass, C.F., and M.D. Albright, 1989: Origin of the Catalina Eddy. *Mon. Wea. Rev.*, **117,** 2406-2436.

Mass, C.F., and G.K. Ferber, 1990: Surface pressure perturbations produced by an isolated mesoscale topographic barrier. Part I: General characteristics and dynamics. *Mon. Wea. Rev.*, **118,** 2579-2596.

Orlanski, I., 1975: A rational subdivision of scales for atmospheric processes. *Bull. Amer. Meteor. Soc.*, **56,** 527-530.

Phillips, N.A., 1957: A coordinate system having some special advantages for numerical forecasting. *J. Meteor.*, **14,** 184-185.

Schultz, P., and T.T. Warner, 1982: Characteristics of summertime circulations and pollutant ventilation in the Los Angeles Basin. *J. Appl. Meteor.*, **21,** 672-682.

Schulz, W.J., 1992: Wind speed and moisture sensitivity tests of the NRL Limited Area Dynamical Weather Prediction Model: An OSSE study of ERICA IOP-4. M.S. thesis, Meteorology Department, Naval Postgraduate School, Monterey, CA 93943.

Streed, D.H., 1990: High-frequency meteorological phenomena observed with the Naval Postgraduate School's UHF doppler wind profiler. M.S. thesis, Meteorology Department, Naval Postgraduate School, Monterey, CA 93943.

Ulrickson, B.L., and C.F. Mass, 1990: Numerical investigation of mesoscale circulations in the Los Angeles Basin. Part I: A verification study. *Mon. Wea. Rev.*, **118**, 2138-2161.

Willmott, C.J., S.G. Ackleston, R.E. Davis, J.J. Feddema, K.M. Klink, D.R. Legates, J. O'Donnell and C.M. Rowe, 1985: Statistics for the evaluation and comparison of models. *J. Geophys. Res.*, **90**, 8995-9005.

INITIAL DISTRIBUTION LIST

		No. Copies
1.	Defense Technical Information Center Cameron Station Alexandria, VA 22304-6145	2
2.	Library, Code 52 Naval Postgraduate School Monterey, CA 93943-5002	2
3.	Chairman (Code MR/Hy) Department of Meteorology Naval Postgraduate School Monterey, CA 93943-5000	1
4.	Chairman (Code OC/Co) Department of Oceanography Naval Postgraduate School Monterey, CA 93943-5000	1
5.	Professor Teddy R. Holt (Code MR/Ht) Department of Meteorology Naval Postgraduate School Monterey, CA 93943-5000	1
6.	Professor Wendell A. Nuss (Code MR/Nu) Department of Meteorology Naval Postgraduate School Monterey, CA 93943-5000	1
7.	Dr. Richard Hodur Naval Research Laboratory-Monterey Monterey, CA 93943-5006	1
8.	Dr. John Hovermale Naval Research Laboratory-Monterey Monterey, CA 93943-5006	1
9.	Dr. Paul Tag Naval Research Laboratory-Monterey Monterey, CA 93943-5006	1
10.	Dr. Simon Chang Naval Research Laboratory Code 4220 Washington, D.C. 20375	1

11. LCDR Frank J. Grandau 1
Naval Western Oceanography Center
Box 113
Pearl Harbor, HI 96860-5050